Progress in Oceanography 185 (2020) 102320

Contents lists available at ScienceDirect

Progress in Oceanography

journal homepage: www.elsevier.com/locate/pocean

Climate effects on temporal and spatial dynamics of phytoplankton and zooplankton in the Barents Sea

Padmini Dalpadado[a,*], Kevin R. Arrigo[b], Gert L. van Dijken[b], Hein Rune Skjoldal[a], Espen Bagøien[a], Andrey V. Dolgov[c,d,e], Irina P. Prokopchuk[c], Erik Sperfeld[f]

[a] Institute of Marine Research, PO Box 1870, 5817 Bergen, Norway
[b] Department of Earth System Science, Stanford University, Stanford, CA, USA
[c] Polar branch of the Federal State Budget Scientific Institution "Russian Federal Research Institute of Fisheries and Oceanography" ("PINRO" named after N.M. Knipovich), 6, Academician Knipovich Street, Murmansk 183038, Russia
[d] Federal State Educational Institution of Higher Education "Murmansk State Technical University", (FSEI HE "MSTU"), 13, Sportivnaya Street, Murmansk, 183010, Russia
[e] Tomsk State University, 36, Lenin Avenue, Tomsk, 634050, Russia
[f] Animal Ecology, Zoological Institute and Museum, University of Greifswald, Loitzer Str. 26, 17489 Greifswald, Germany

ARTICLE INFO

Keywords:
Phytoplankton
Bloom dynamics
Mesozooplankton
Capelin predation
Key processes
Climate effects
Barents Sea

ABSTRACT

Temporal and spatial dynamics of phytoplankton and zooplankton in the Barents Sea have been investigated during the last three decades using remote sensing and *in situ* observations. Satellite-derived sea surface temperatures increased in the period 1998–2017 by 1.0 °C as an average for the Barents Sea. We found significant positive relationships between ice-free conditions (open water area and duration) and satellite-based net primary production (NPP). The estimated annual NPP for the Barents Sea more than doubled over the 1998–2017 period, from around 40 to over 100 Tg C. The strong increase in NPP is the result of reduction of sea ice, extending both the area and period available for phytoplankton production. In areas where ice extent has decreased, satellite-derived chlorophyll *a* shows that the timing of the peak spring phytoplankton bloom has advanced by over a month. Our results reveal that phytoplankton dynamics in the ecosystem have been changing rapidly and that this change is driven mainly by bottom-up climatic processes. Autumn mesozooplankton biomass showed strong interannual variability in the 1990s, displaying an inverse relationship with capelin biomass, the most abundant planktivorous fish. In some regions, e.g. Central Bank, capelin biomass explained up to 50% of the mesozooplankton variability during 1989–2017. Though capelin biomass has varied considerably, mesozooplankton biomass has remained rather stable since the mid-2000s (6–8 g dry wt. m^{-2}), resulting in a weakening of the negative relationship between capelin and mesozooplankton biomass in recent years. The stable zooplankton biomass indicates favorable conditions (prolonged/increased NPP) for mesozooplankton production, partly counteracting high predation levels. Overall, we observed trends in phytoplankton phenology that were strongly associated with changes in sea ice cover driven by fluctuations in temperature regime, a trend that may intensify should the ecosystem become even warmer due to climate change. Further reductions of sea ice and associated ice algae is expected to have adverse effects on sympagic fauna and ice dependent species in the Arctic food web. The ice-free conditions may promote further Atlantification (or borealization) of plankton and fish communities in the Barents Sea.

1. Introduction

High latitude seas are cold-water, high-productivity systems that can sustain large fish stocks important for fisheries (ICES/WGIBAR, 2018). Due to climate change, these polar seas are predicted to be particularly affected (Kelly, 2016). Loss of sea ice, warming of ocean waters, and potential changes in the timing of productive seasons have been documented (ICES/WGIBAR, 2018) and are likely to continue in the years to come (Kelly, 2016). Climate change and variability may affect the whole pelagic food web from phytoplankton to zooplankton to higher trophic levels (Kelly, 2016; Reygondeau and Beaugrand, 2011; Richardson, 2008).

The Barents Sea, a high latitude system, is a productive sea supporting some of the world's largest demersal fish stocks such as cod

* Corresponding author.
E-mail address: padmini.dalpadado@hi.no (P. Dalpadado).

https://doi.org/10.1016/j.pocean.2020.102320

Available online 08 April 2020

(*Gadus morhua*) and haddock (*Melanogrammus aeglefinus*) as well as pelagic stocks such as capelin (*Mallotus villosus*) (ICES, 2018). In addition, the ecosystem acts as a nursery ground for spring-spawning herring (*Clupea harengus*) and is home for a variety of marine mammals and large seabird populations (Hunt et al., 2013). The rich and diverse plankton community in the Barents Sea sustains these upper trophic levels (Eriksen et al., 2017; Hunt et al., 2013). Key copepod species *Calanus finmarchicus* and *C. glacialis*, as well as krill (euphausiids) *Thysanoessa inermis* and *T. raschii*, are regarded as predominantly herbivorous (Dalpadado et al., 2008; Dalsgaard et al., 2003), allowing an efficient trophic transfer of energy from phytoplankton to fish (e.g. Dalpadado et al., 2014).

The Barents Sea is a large Arctic shelf sea that connects with the deeper Norwegian Sea to the west, the Arctic Ocean to the north, the Kara Sea to the east, and borders the Norwegian and Russian coasts to the south. It covers an area of approximately 1.6 million km^2, has an average depth of 230 m, and a maximum depth of about 500 m at the western end of Bear Island Trench. The dynamics of the system are greatly dependent on the inflowing warm Atlantic currents from the Norwegian Sea to the west and Arctic waters entering from the north (Dalpadado et al., 2012; ICES/WGIBAR, 2018). The variability in ice cover is an important process (Loeng, 1991), imposing great consequences for the biological development in this region (Skjoldal and Rey, 1989). In general, large areas of the region are covered with sea ice during winter while the southern parts with inflow of Atlantic water remain open. A large but variable part of the Barents Sea is influenced by seasonal ice. The ice cover variation in the Barents Sea is caused by fluctuations in large-scale atmospheric and oceanic circulation, the amount of heat transported with inflowing Atlantic water, and the river run-off from land (Årthun et al., 2012; Lind et al., 2018; Onarheim et al., 2015; Vinje, 2009). The amount of sea ice in the Arctic has dropped by approximately 9% per decade since 1978 and has been accompanied by reduced sea ice thickness and duration (Arrigo and van Dijken, 2015; Carmack et al., 2015; Polyakov et al., 2017).

The total annual primary production for the Barents Sea has been estimated to be around 70–100 g C m^{-2}, with higher rates for the open Atlantic waters in the southern parts and lower rates for the ice-covered waters in the northern Barents Sea (Hunt et al., 2013; Reigstad et al., 2011; Sakshaug, 2004; Wassmann et al., 2006a). The phytoplankton spring bloom in the Atlantic water domain without sea ice is thermocline-driven, whereas in the Arctic domain with seasonal sea ice, stability from melting ice determines the timing of the ice edge phytoplankton bloom (Hunt et al., 2013; Sakshaug and Skjoldal, 1989; Skjoldal and Rey, 1989). Significant trends towards earlier blooms have been detected in about 11% of the area of the Arctic seas, e.g. in Hudson Bay, Foxe Basin, Baffin Sea, off the coasts of Greenland, in the Kara Sea, waters around Novaya Zemlya, and in the Arctic domain of the Barents Sea (Kahru et al., 2011). Ice algae, which grow on the underside of sea ice, play a small role for the overall primary production in the Barents Sea (Hegseth, 1998; Hunt et al., 2013; Wassmann et al., 2006b), although they are relatively important in terms of seasonal phenology and reproduction of Arctic copepods (Leu et al., 2011; Søreide et al., 2010). A study by Wang et al. (2015) in the Bering Sea showed that organic matter originating from sea ice algae was present in key zooplankton organisms such as the pelagic amphipod *Themisto libellula* (36 to 72%), *C. marshallae/glacialis* (27 to 63%), and *T. raschii* (39 to 71%). Lipid and isotope analyses from the central Arctic Ocean revealed substantial, but varying ice algae origin for *Apherusa glacialis* and other sympagic (ice-associated) amphipods, the pelagic copepods *C. glacialis* and *C. hyperboreus*, and the pelagic amphipod *T. libellula* (Kohlbach et al., 2016).

Zooplankton biomass in the Barents Sea can show large interannual variability, driven by both top-down and bottom-up processes (Kvile et al., 2014; Orlova et al., 2010a; Skjoldal et al., 1992; Stige et al., 2014). *Calanus* species are main drivers of variation in the mesozooplankton biomass in the Barents Sea, and they constitute around 80% of the total biomass (Aarflot et al., 2018). Though *Calanus* species co-occur in most regions, *C. finmarchicus* dominates in Atlantic waters while *C. glacialis* dominates in the Arctic water masses (Aarflot et al., 2018; Dalpadado et al., 2012; Melle and Skjoldal, 1998). These studies also show that the larger *C. hyperboreus* has considerably lower biomass in the Barents Sea than the other two *Calanus* species. Horizontal and vertical distributions of zooplankton biomass determine feeding conditions for pelagic planktivorous fishes in the Barents Sea such as young herring, capelin, and polar cod (*Boreogadus saida*), as well as pelagic 0-group of cod and haddock, and seasonally distributed blue whiting (*Micromesistius poutassou*).

Capelin represents the largest pelagic fish stock in the Barents Sea, and it is a key player in the Arctic food web due to its dual role (Gjøsæter, 1998). While being a key predator on the zooplankton, the capelin in years with a large stock-size constitutes the main food source of cod (Bogstad et al., 2015; Dalpadado and Mowbray, 2013; Dolgov et al., 2011; Gjøsæter et al., 2000; Orlova et al., 2010a). Hassel et al. (1991) reported that if capelin consumes 10% of its body weight per day, the zooplankton will be depleted in only 3–4 days where the capelin is heavily concentrated. The diet of smaller capelin is dominated by copepods, whereas for larger individuals, euphausiids can be a key dietary item (Dalpadado and Mowbray, 2013; Dolgov et al., 2011; Orlova et al., 2010b). During the last decade, there has been a general expansion of the distribution and a northward shift of the high-concentration areas of capelin, which has been related to the high temperatures and low ice cover observed in the northern Barents Sea during this period (Ingvaldsen and Gjøsæter, 2013). Boreal zooplankton and fish species are likely to expand their distributions further north and east, exploiting the improved habitat conditions, and some of these changes have already been reported (Eriksen et al., 2016, 2017; Fossheim et al., 2015; ICES/WGIBAR, 2017, 2018).

The main goal of this study is to better understand the dynamics of phytoplankton and mesozooplankton in an era of warming, and their interactions with capelin as the most abundant planktivorous fish in the ecosystem, through exploration of various spatially and temporally resolved data sets (Supplementary Table 1). The focus of the current work is to investigate: 1) spring and autumn phytoplankton bloom dynamics, 2) spatial and interannual variability in net primary production (NPP), 3) spatial and seasonal distribution patterns of chlorophyll *a* (Chl *a*) and mesozooplankton, and 4) key bottom-up and top-down processes regulating plankton dynamics.

2. Material and methods

2.1. Spatial data and polygon division

In the current study, the Barents Sea was divided into 15 polygons to explore spatial variability mainly based on topographical conditions (Fig. 1, ICES/WGIBAR, 2018). The three largest banks are Central Bank, Great Bank, and Svalbard Bank (represented in the Svalbard South polygon). Several troughs deeper than 300 m run from the central Barents Sea to the northern (e.g. Franz Victoria Trough) and western (e.g. Bear Island Trench) continental shelf break. The western trough allows influx of Atlantic waters to the central Barents Sea (ICES, 2016).

2.2. Satellite-derived remote sensing (1998–2017)

Remote sensing data with high spatial and temporal resolution were used to obtain Chl *a* concentration (mg m^{-3}), mean daily NPP (g C m^{-2} day^{-1}), spatially-integrated NPP (Tg C day^{-1}), open water area (OWA, km^2), open water duration (OWD, number of days) and sea surface temperature (SST, °C) for each of the polygons on a yearly basis. Daily NPP, OWA, and OWD were calculated from satellite data as described in detail in Arrigo and van Dijken (2015). Satellite-derived surface Chl *a* (Sat Chl *a*, Level 3, 8 days binned, reprocessing version R2018.0) was based on SeaWiFS and MODIS/Aqua sensors. SeaWiFS was used in

Fig. 1. Division of the Barents Sea into 15 polygons, mainly based on topographical conditions. Red lines show locations of standard oceanographic sections at the Fugløya-Bear Island (FB) section at the western entrance to the Barents Sea (IMR, Norway) and the Kola section (PINRO, Russia).

1998–2002, and MODIS/Aqua in 2003–2017. For the years where data were available for both sensors (2003–2007), SeaWiFS Chl *a* was consistently higher than MODIS/Aqua concentrations. Therefore, we used a correction factor for SeaWiFS Chl *a* to create a comparable 20-year time series. Chl *a* concentration per polygon was calculated as the mean of all valid Chl *a* pixels within a polygon, excluding non-valid pixels caused by clouds or ice. The values for the South-East and Pechora polygons were recalculated excluding the regions most influenced by river inflow (18% and 41% of the total area, respectively). Start of phytoplankton bloom is based on two definitions: a threshold Chl *a* concentration of 0.5 mg m^{-3} and a fraction of 0.3 to the maximum Chl *a* level. Spring and fall blooms are defined respectively as before and after 31 July. Open water duration is the number of days where the open water area of a polygon is >50% of the total area of the polygon.

Validation of satellite Chl *a* using *in situ* data showed significant correlations between the two variables in the Barents Sea (Dalpadado et al., 2014; ICES/WGIBAR, 2017, this study) and thus, the NPP model based on satellite data by Arrigo et al. (2008, 2015) gives reasonable results that compare well with sea ground truthing measurements. Dalpadado et al. (2014) used *in situ* Chl *a* data in the upper 20 m and 50 m to validate the time series of satellite based Chl *a* concentrations at the Fugløya-Bear Island (FB) section for the period 1998–2011. Their results showed that the seasonal dynamics and magnitude of the satellite Chl *a* concentrations are strongly correlated with the observed Chl *a* concentrations both for the upper 20 m and 50 m. Also, estimates of new production of phytoplankton based on nitrogen consumption (seasonal draw-down of nitrate in the water column) for the FB and Vardø-Nord (VN) sections, representing the western and central Barents Sea respectively, from March to June (includes spring and summer production) resulted in values comparable to satellite NPP estimates (Rey, F., pers. com.).

2.3. *In situ* Chl *a*, nutrients, and mesozooplankton sampling

Broad-scale surveys of the Barents Sea ecosystem are carried out annually in the autumn jointly by the Institute of Marine Research (IMR) in Norway and the Polar Research Institute for Marine Fisheries and Oceanography (PINRO, since 2019 named as Polar branch of Russian Federal Research Institute of Fisheries and Oceanography) in Russia (Eriksen et al., 2018). In addition to monitoring of fish and hydrography, the surveys monitor and map the horizontal and vertical distributions of Chl *a*, nutrients, and zooplankton over an area of >1 million km^2. The survey is carried out in late summer and autumn (August-October) when open water has the maximum extent and much of the northern, Arctic part of the Barents Sea is available for sampling with regular research vessels.

2.4. *In situ* Chl *a* and nitrate measurements at the FB section (1987–2017)

IMR has monitored Chl *a* (0–100 m), nitrate and other nutrient concentrations along the FB section regularly covering most seasons since the early 1980s. This section (approx. 20 stations) covers the western opening to the Barents Sea and crosses three different water masses (Coastal, Atlantic, and mixed Atlantic/Arctic). It provides information on the seasonal development of phytoplankton and nutrients (e.g. Chl *a* and nitrate).

Water samples for analyses of nutrients and Chl *a* were obtained at predefined depths (5, 10, 20, 30, 50, 75, 100, 150, 200, 300, 400, and

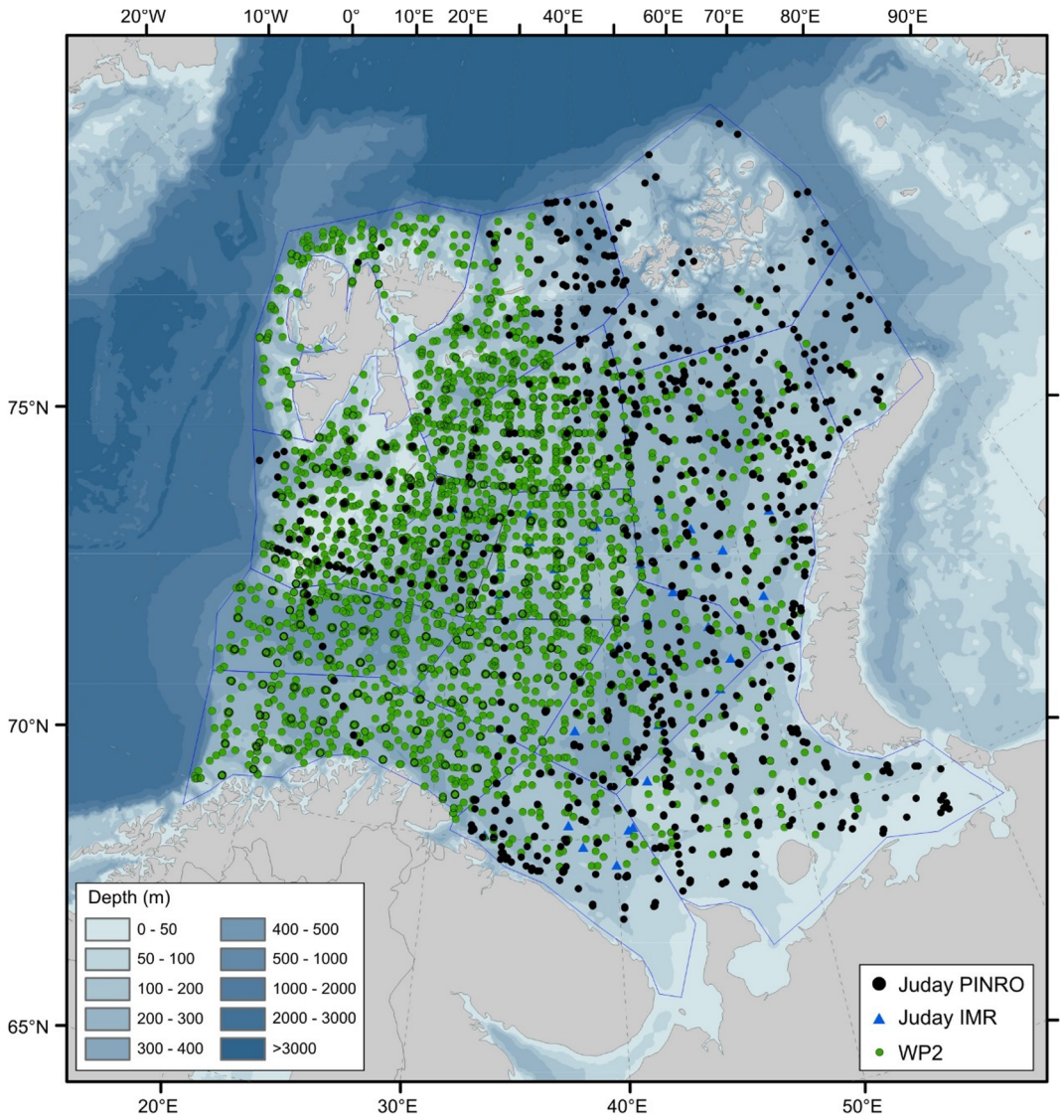

Fig. 2. Locations of mesozooplankton sampling in joint IMR and PINRO autumn (August to early October) ecosystem surveys during 1989–2017.

500 m) and later measured in the laboratory. Nutrient samples (20 ml) were collected in plastic vials and preserved with 0.2 ml chloroform and kept at 4 °C (Hagebø and Rey, 1984). These samples were analysed with an auto-analyzer using standard methods (Strickland and Parsons, 1972). Water samples (263 +/− 3 ml) for Chl *a* analyses were filtered onboard the ship using glass-fiber filters (GF/C) and kept frozen (−18 °C) until later analyses. In the laboratory, the pigments on the filter were extracted overnight with 90% acetone at 4 °C. After centrifuging the extracts, Chl *a* was measured by fluorometry before and after acidification using standard methods (Aminot and Rey, 2000).

2.5. Water temperature on the Kola section

Temperature data from the Kola section were obtained from ICES/WGIBAR (2017, 2018); see also the PINRO website (http://www.pinro.ru/labs/hid/kolsec22.php). We have used the mean of the 2015 and 2017 values for the missing year 2016. Kola temperature shows remarkable similarity to the Atlantic Multi-Decadal Oscillation (AMO) index, demonstrating that the climate variation found in this section is a local manifestation of larger-scale climate fluctuations covering the entire North Atlantic (Skagseth et al., 2008).

2.6. Water mass area

The area of Atlantic water (AW), Arctic water (ArW), and mixed waters were extracted from ICES/WGIBAR (2017, 2018) reports. The area of each water mass in the Barents Sea was classified using temperature values. Temperature data collected using a CTD (conductivity, temperature, depth) system during the annual autumn surveys have been interpolated into horizontal grids with 1/6° meridional resolution (18 km). From the gridded fields, mean temperature fields in the 50–200 m depth range were calculated, and the areas and mean temperature of AW (>3°C), ArW (<0°C), and mixed waters (0–3 °C) were estimated. Refer to Dalpadado et al. (2012) for more details. Only the area of ArW was used in correlation analyses of this study.

2.7. Mesozooplankton

Mesozooplankton biomass was monitored using WP2 and Juday nets on the joint ecosystem autumn surveys (August to early October; Fig. 2). Intercalibration of the two nets was conducted in August 2013 on board the IMR RV “Johan Hjort”. Total biomass samples obtained with the two nets at a given speed (0.5 m s^{-1} or 1 m s^{-1}) and analyzed in the same way were comparable with differences amounting to ~14% (Skjoldal et al., 2019, see also Skjoldal et al., 2013). WP2 and Juday

samples showed a strong covariation and similar biomass and species composition patterns (Skjoldal et al., 2019). Hence, data from both types of gears were combined to explore interannual and spatial variability in mesozooplankton biomass.

2.8. WP2 net sampling (1989–2017)

The WP2 used by IMR is a simple standard net (0.56 m opening diameter, mesh size 180 μm), which was towed vertically from near the bottom to the surface. The net was rinsed, and the sample was collected in the cod-end and treated according to the standard IMR procedure (see Melle et al., 2004; Skjoldal et al., 2013). The total sample content was transferred to a Motoda plankton splitter and divided into two halves: one for biomass determination and the other for taxonomic analysis and species enumeration. The biomass sample was screened successively through three meshes: 2 mm, 1 mm, and 180 μm. The content on each screen was briefly rinsed with freshwater to remove salt and transferred to pre-weighed aluminum trays. The samples were dried at 60 °C for >24 h and then frozen at −20 °C. In the laboratory on shore, the samples were once more dried at 60 °C before weighed. The sum of the three fractions (i.e. total biomass) was used in this study to allow comparison with data from PINRO that are not size-fractioned.

2.9. Juday net sampling (1989–1990; 2001–2017)

A Juday net (0.37 m opening diameter, 180 μm mesh size) was used by IMR during 1989–1990 (for a limited number of samples in those years) and by PINRO during 2001–2017. The net was towed vertically from close to the bottom to the surface. With the PINRO procedure, the whole samples were preserved in 4% formaldehyde and later rinsed and weighed at the laboratory for biomass determination. The PINRO wet weight biomass was converted to dry weight by dividing by a factor of 5 (Kiørboe, 2013; Skjoldal et al., 2004).

The biomass, collected by WP2 and Juday nets, integrated over the entire water column was calculated by using the area filtered (net mouth opening) and expressed as g dry wt. m^{-2}.

2.10. Capelin biomass

Biomass of capelin (one year and older) was based on acoustic estimates from autumn ecosystem surveys in the Barents Sea and was extracted from ICES (2018).

3. Data analyses

Correlation analyses were performed using the mean values for each year to explore relationships between the time series of physical (satellite-derived SST, Kola section temperature, OWA) and biological (NPP, Chl *a*, mesozooplankton biomass, and capelin biomass) variables. The strength of a correlation between two time series was estimated by the Pearson correlation coefficient (r), and significance was tested while correcting for autocorrelation in the two-time series as well as correcting for multiple comparisons using Bonferroni correction. To account for autocorrelation, the effective number of degrees of freedom (i.e. the number of independent joint observations, Nc = d.f. + 2) in significance tests of correlations was adjusted following a method proposed by Quenouille (1952) and modified by Pyper and Peterman (1998), using equations summarized by Dalpadado et al. (2012). Trends in the physical and biological variables over time (years) were described by Pearson correlation coefficients without correcting for autocorrelation in significance tests. Analysis of Covariance (ANCOVA) was used to test whether SST changed over the years (1998–2017) across polygons.

Linear regressions of SST over time for each polygon were used to identify the polygons that showed a significant temperature increase with time. A non-parametric Mann–Whitney test was performed to reveal whether there were significant differences between time periods (before and after 2004) of the mesozooplankton biomass of the Thor Iversen Bank, Great Bank, and Central Bank polygons during 1989–2017.

Principal component analysis (PCA; Legendre and Legendre, 2012) was used to show how Barents Sea polygons were related to different biotic and abiotic variables. For each variable, we used the average of all years per polygon; data were centered and scaled for calculating principal components. The analysis was performed using the function “prcomp” of the “R” software (R Core Team, 2018).

4. Results

4.1. Sea surface temperature

Remote sensing data showed that there was an increasing trend in mean annual SST in most of the polygons of the Barents Sea during 1998–2017 (Fig. 3A; ANCOVA, year: $F_{1,270} = 226.2$, $p < 0.001$, polygon: $F_{14,270} = 766.8$, $p < 0.001$), with only 2 polygons not showing a significant increase (FVT and FJL, Supplementary Table 2). The increase in SST differed among polygons (ANCOVA, year × polygon interaction: $F_{14,270} = 6.3$, $p < 0.001$; Supplementary Table 2). In general, SST was the highest in regions influenced by the warm Atlantic Current (South West, Bear Island Trench, Thor Iversen Bank and South East) whereas the lowest SST was observed in the northernmost polygons (St. Anna Trough, Franz Joseph Land) influenced by the Arctic waters. Polygons in the east, such as the Pechora Sea and South East Basin, showed the highest rate of increase in SST (Supplementary Table 2), corresponding to a total warming of 2.2 and 2.1 °C, respectively, during the 20-year study period. The warming trend was on average 0.055 °C y^{-1} (SD 0.035), corresponding to an increase of 1.0 °C over the 20-year period (varying from 0.5 to 2.2 °C for the polygons showing a significant increase). This magnitude of warming is in general agreement with hydrographic observations during the autumn surveys (ICES/WGIBAR, 2017).

4.2. Open water area (OWA)

The maximum OWA in late summer or autumn in the Barents Sea estimated by remote sensing has significantly increased over the years due to reduction of sea ice. The increase has been by nearly 320,000 km^2 over the 20-year time series (16,840 km^2 y^{-1}), which represents about 20% of the total area of the Barents Sea (1.6 million km^2). Polygons in the southern Barents Sea experienced permanently open water or just some slight ice since the beginning of the time series (see straight lines in Fig. 3B). For the polygons in the central and northern Barents Sea, there have been progressively larger OWAs, most pronounced for the North-East.

4.3. Spatial and temporal patterns of Chl a in spring

Remote sensing data were used to explore the seasonal and interannual variability in Chl *a* distribution. Satellite data from the Barents Sea during 1998–2017 showed large interannual variability, with the highest Chl *a* concentrations generally observed in May (Fig. 4; not shown for all months and years). It should be noted that satellites can detect the color from Chl *a* only in open water, since even low amounts of ice (down to ~10% areal coverage) mask the signal from ocean color. A comparison of the Chl *a* distribution pattern for a ‘cold year’ (1998) versus a ‘warm year’ (2016) with less sea ice shows north- and eastward expansion of the distribution, with earlier blooming and higher concentrations in the eastern regions in the ‘warm year’ (Fig. 4). The year 2017 was a colder year with more ice compared to 2016. Though the Chl *a* distribution pattern was somewhat similar, the spring bloom Chl *a* was much lower during April to June in 2017 compared to the previous year.

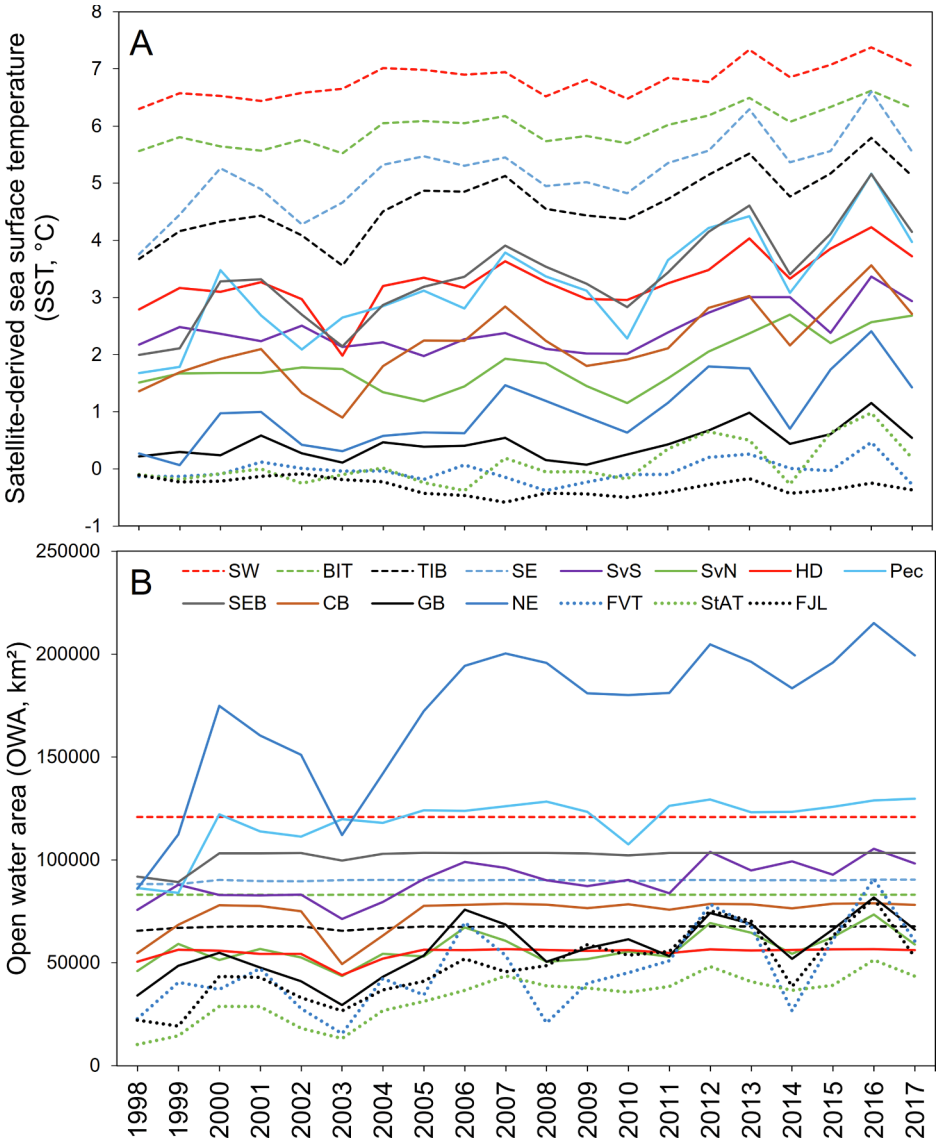

Fig. 3. Interannual variability in (A) sea surface temperature (SST) and (B) open water area (OWA) for the different polygons in the Barents Sea estimated by satellite remote sensing. South West (SW), Bear Island Trench (BIT), Thor Iversen Bank (TIB), Hopen Deep (HD), Svalbard South (SvS), Svalbard North (SvN), South East (SE), Pechora Sea (Pec), Southeastern Basin (SEB), Central Bank (CB), Great Bank (GB), Franz Victoria Trough (FVT), North East (NE), St. Anna Trough (StAT), Franz Joseph Land (FJL). The straight lines in (B) indicate polygons for which the whole area is open water throughout the whole year; note that the values for the South-East and Pechora polygons were recalculated excluding the regions most influenced by river inflow (18% and 41% respectively), hence excluding some of the ice covered area. Dashed lines indicate open water polygons with mostly no ice throughout the year, solid lines indicate seasonally ice covered polygons, and dotted lines indicate more heavily ice covered polygons.

4.4. Seasonal dynamics of Chl a concentration – spring and fall (autumn) blooms

The seasonal dynamics of Chl *a* showed an increase starting in late winter to a pronounced peak which represents the spring bloom (Fig. 5). We grouped the polygons into three categories: i) permanently open water, ii) seasonal ice-cover, where most or all of the polygon area clears of ice during summer, and iii) heavier ice-cover, where some ice remains through summer. The spring phytoplankton bloom was a distinctive feature, as seen from satellites in open water polygons and polygons with seasonal ice cover (Fig. 5A, B), but was less distinct in polygons with heavier ice cover (Fig. 5C). Following the spring bloom, Chl *a* levels were generally low in summer. The increase in autumn, commonly referred to as 'autumn bloom', was slight and most clearly seen in the open water polygons (Fig. 5A).

The maximum Chl *a* concentration in spring was generally much higher (average ~3.0 mg m^{-3}) than in autumn (<1 mg m^{-3}). At the polygon level, the spring bloom peak was the highest in the South East Basin (~5 mg m^{-3}) and lowest in Franz Victoria Trough (0.8 mg m^{-3}) (Fig. 6A; Supplementary Table 3). There was a clear spatial pattern with higher average spring peak Chl *a* for southern and central polygons (1.5–5 mg m^{-3}) compared to northern polygons (1–1.5 mg m^{-3}) (Fig. 6A). There was large interannual variability in the magnitude of the spring bloom over the years (Supplementary Table 3), reflected in coefficients of variation (CV = SD/mean) between 0.37 and 0.89 for the different polygons.

The average timing of the spring bloom peak varied by up to 50 days among the polygons, with early blooming in the South West region (day of the year, DOY = 130; 10 May) and late blooming in the northern polygons, e.g. Franz Victoria Trough (DOY = 180; 29 June) and Franz Joseph Land (DOY = 175; 24 June). The spring bloom peak in the open water (South West, Bear Island Trench, Thor Iversen Bank, South East) or mostly open water (Hopen Deep, Southeastern Basin) polygons (see Fig. 3B) occurred on DOY 130–145, or 10–25 May (Fig. 6B). In the polygons with seasonal and variable sea ice conditions (Central Bank, Great Bank, North East, Svalbard South, Svalbard North) the peak bloom occurred on DOY 140–151, or 20–31 May.

The start of the spring bloom was strongly correlated with the timing of the peak bloom (R^2 = 0.91; Fig. 6B). The time from start to peak was typically around 4 weeks for the open water polygons (23–29 days) and the polygons with seasonal sea ice (19–45 days), while being shorter (about 2–3 weeks) for the northernmost polygons (12–20 days; Fig. 6B). The first detectable increase in Chl *a* occurred as early as DOY 80–90, or about 20–30 March, in open water and seasonally ice-covered polygons (Fig. 5A, B; Supplementary Table 4). This reflects the early growth of phytoplankton in the pre-bloom stage,

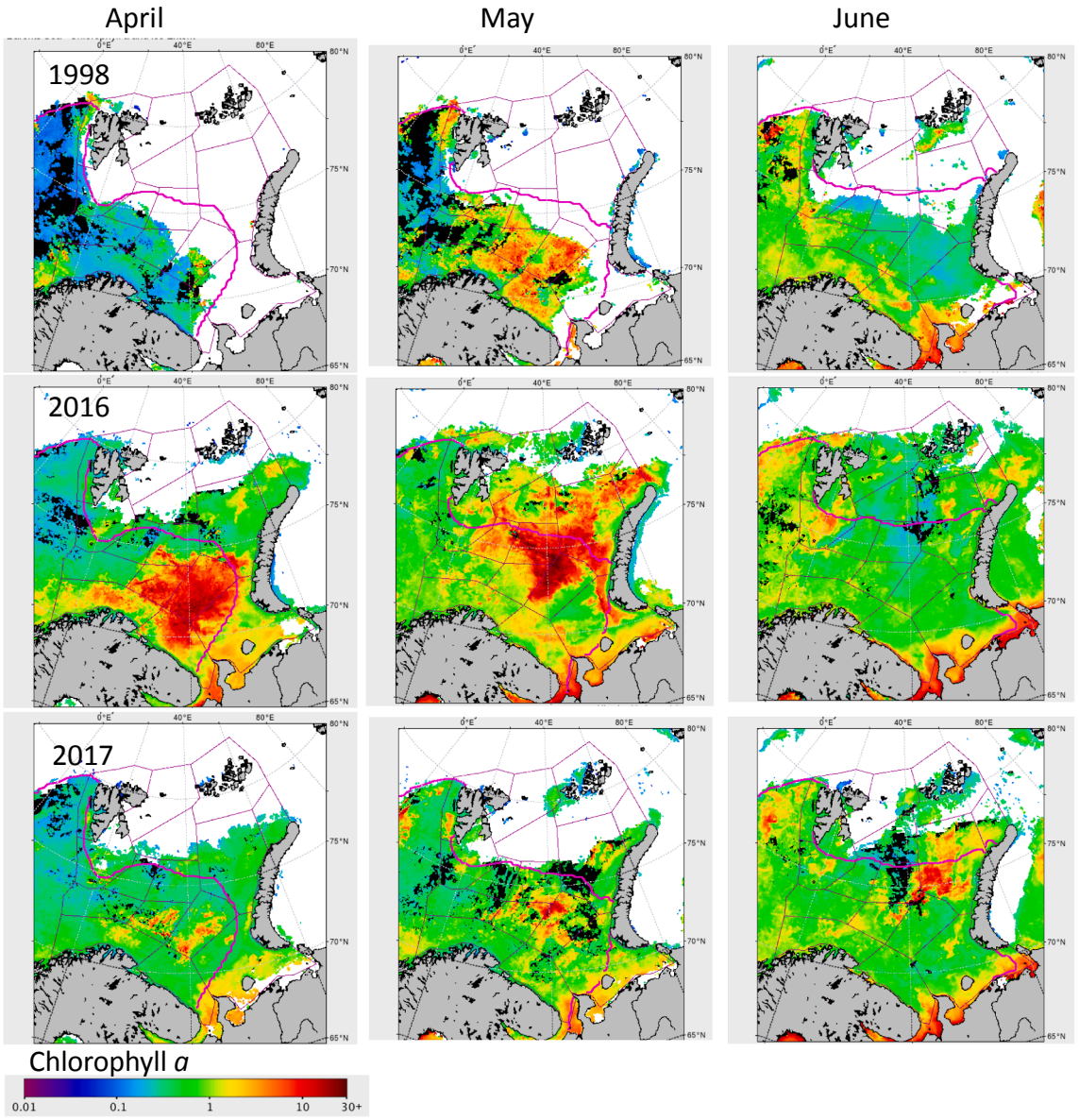

Fig. 4. Spatial distributions of Chl *a* (mg m^{-3}) in April, May, and June for 1998 (cold year; upper panels), 2016 (warm year; middle panels), and 2017 (moderate warm year; lower panels). White areas indicate ice-coverage. The pink lines show the climatological (average 1981–2010) position of the ice edge. Black areas indicate no observations.

starting already at around the time of the spring equinox.

The Chl *a* fall peak showed higher values in the open water polygons (1.0–1.2 mg m^{-3}) and often values <1.0 mg m^{-3} in the seasonal ice and northern polygons (0.4–0.7 mg m^{-3}); the Svalbard polygons were intermediate (0.8–0.9 mg m^{-3}) (Fig. 6A, Supplementary Table S3). The timing of the fall peak varied less (up to 25 days) compared to the spring bloom peak. There was also a spatial pattern in fall timing but opposite to that in spring, with later peak timing for the open water polygons (DOY 239–250, or 27 August–7 September) and earlier timing (by about two weeks) for the northern polygons (DOY 225–233, or 13–21 August) (Fig. 6B). Of the polygons with seasonal ice, Hopen Deep, Central Bank and North East tended to group with the open water polygons (later peak), while Great Bank and the Svalbard polygons grouped with the northern polygons (earlier peak).

The spring peak Chl *a* level had a dominant influence on the seasonally averaged (March-September) Chl *a* concentration, reflected in a high positive correlation between the two measures ($r = 0.80$). The spring peak Chl *a* was about 8 times higher than the seasonal mean. The autumn peak Chl *a* was not correlated with the spring peak level ($r = -0.07$).

The spring bloom started progressively earlier over time as an average over all the polygons; this was statistically significant when based on the fraction (0.3) ($p = 0.004$) as well as when using the absolute threshold definitions. This was driven by a trend for the northern and most ice-influenced polygons (Franz Victoria Trough, St. Anna Trough, Franz Joseph Land), where the spring bloom started 5 weeks earlier in 2017 than in 1998 based on the trendline for the time series (Fig. 7). Open water polygons and polygons with seasonal ice cover did not show a statistically significant trend over the study period (1998–2017, Fig. 7). Similar trends were found for the timing of the spring bloom peak, which occurred about 3 weeks earlier for the northern polygons (not shown).

The fall bloom occurred earlier in the northern than in the central and southern Barents Sea (Fig. 6B). The term 'bloom' may not be quite appropriate, as this is a rather modest increase in Chl *a* (to mean peak levels of around 0.4–1.3 mg m^{-3}; Fig. 6A) in response to an increased availability of nutrients at the beginning of autumn vertical mixing. The productive season is shorter in the north than in the south, as seen from

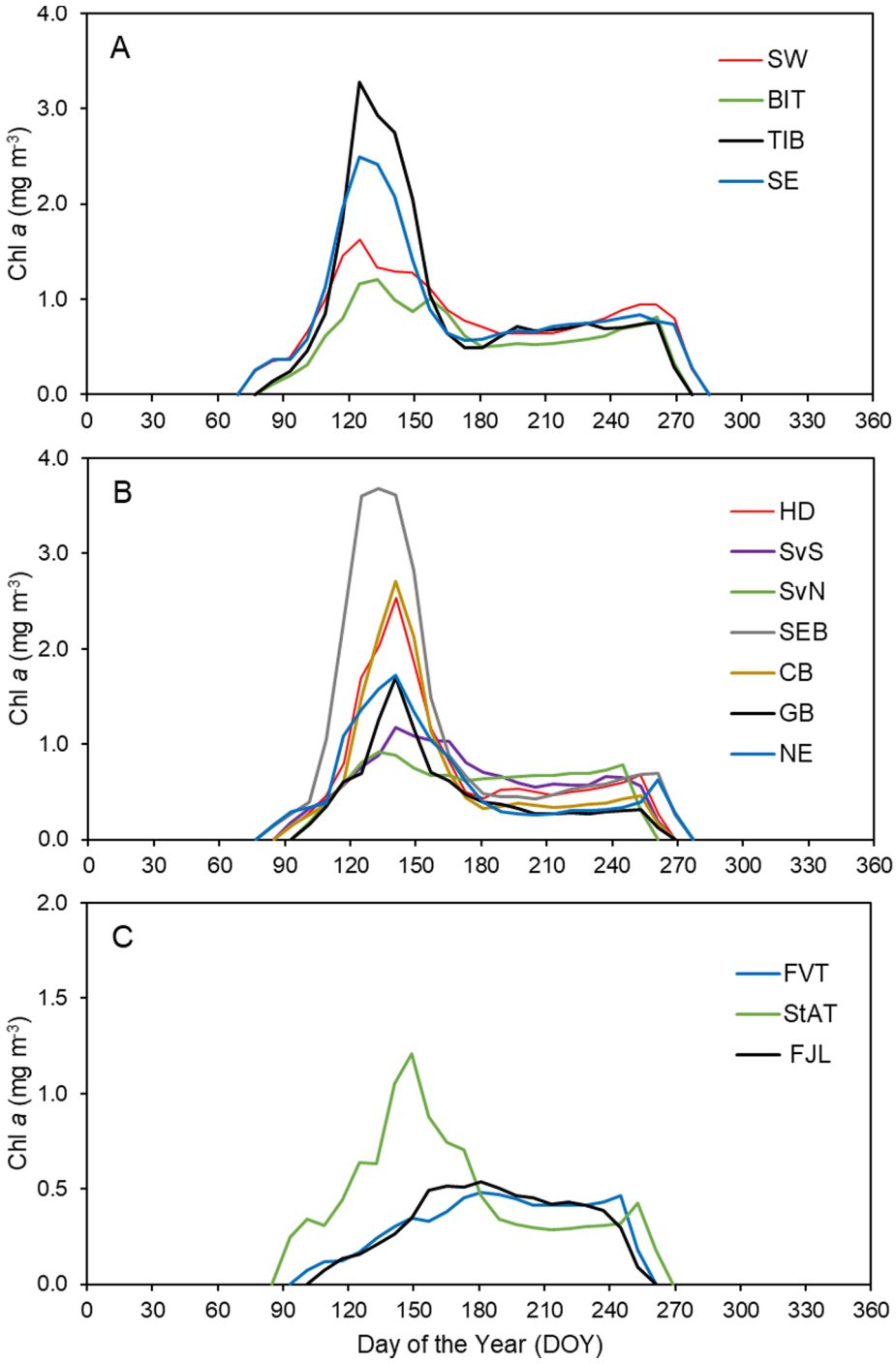

Fig. 5. Mean seasonal pattern (climatology 1998–2017) of satellite-derived Chl *a* concentration in different polygon classes: open water areas with no ice (A), seasonally ice-covered areas (B), and more heavily ice-covered areas (C). Note that the values for the South-East polygon were recalculated excluding the regions most influenced by river inflow (18% of polygon area). See Fig. 1 for location and legend to Fig. 3 for name abbreviations of the polygons. Note different scales on y-axis.

the shorter interval between peak spring and peak fall blooms (Fig. 6B). This reflects a later spring bloom in the north compared to the south due to sea ice, and a truncation of phytoplankton growth in fall due to a more rapid decline in light associated with the approaching polar night at higher latitude.

4.5. Seasonal dynamics of Chl a, nitrate and zooplankton at the FB section

Seasonal dynamics of Chl *a*, nitrate, and zooplankton biomass at the FB section were examined for two periods, 1987–1999 and 2000–2017 (Fig. 8). The latter period was warmer (cf. Fig. 3A). As the temporal coverage varied slightly from year to year, the data for the different years were pooled to achieve better monthly resolution. Chl *a* concentration was very low in winter (January-March) in both periods, with the average for the 0–20 m stratum usually being below 0.02 mg m^{-3}. The spring Chl *a* concentration was higher and displayed a steeper increase during 2000–2017 than during 1987–1999, e.g. April concentrations were 0.3 mg m^{-3} in 1987–1999 compared to 0.7 mg m^{-3} in 2000–2017. The Chl *a* concentration during the fall peak was lower than in spring. The monthly data averaged for the period

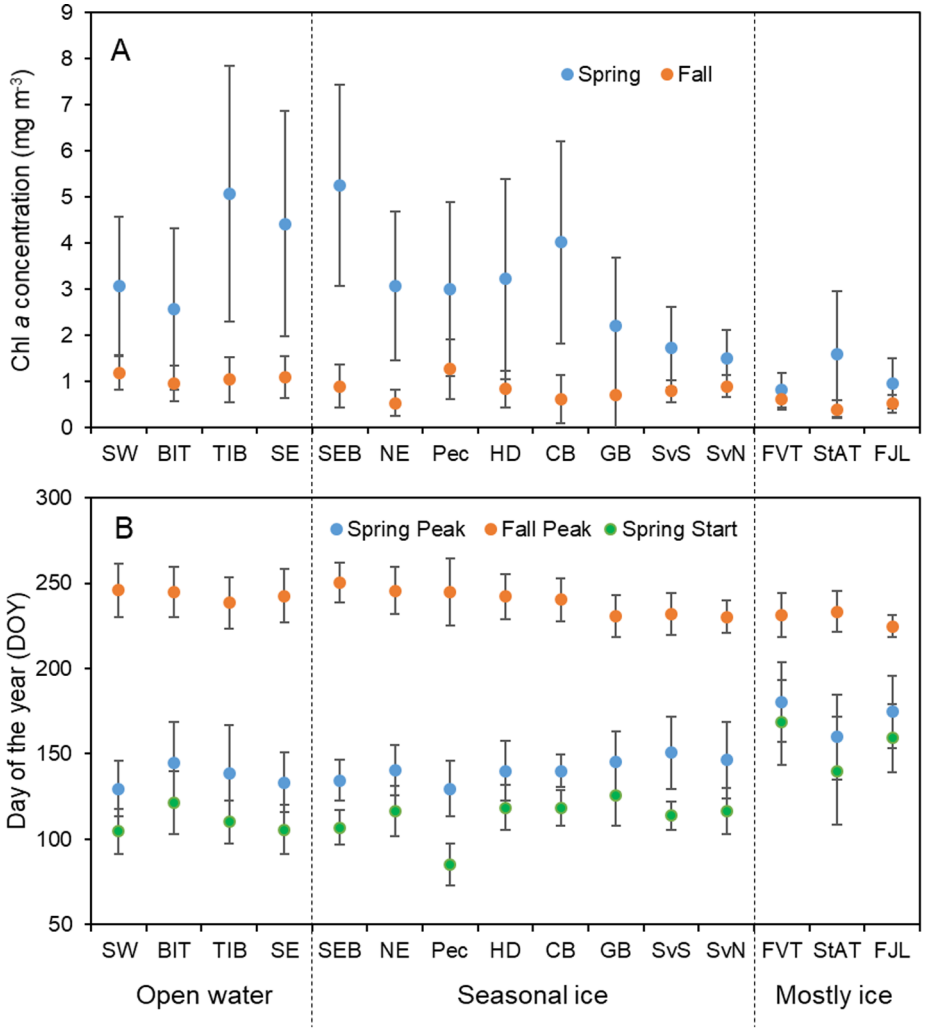

Fig. 6. Spatial patterns of peak Chl *a* (A) and timing (B) of spring and fall blooms by polygons. See Fig. 1 for location and legend to Fig. 3 for name abbreviations of the polygons. Mean values (points) and +/− standard deviation (error bars) for satellite-derived estimates for 1998–2017 (n = 20). Timing is given as Day-of-Year for peak spring bloom, start spring bloom (reaching maximum Chl *a* concentration and a threshold of 0.5 mg m^{-3}, respectively), and peak fall bloom (maximum Chl *a* concentration after 1 July).

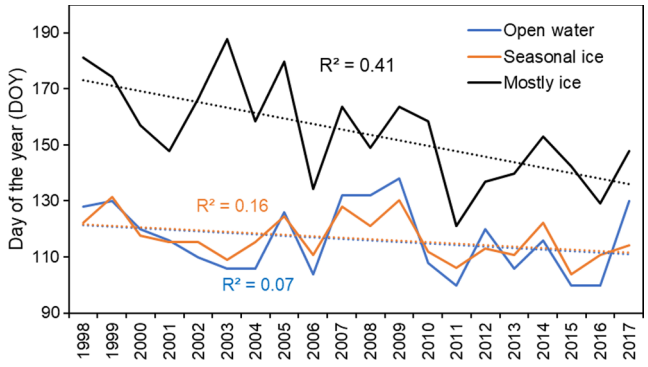

Fig. 7. Timing (Day-of-Year) for the start of the spring bloom (reaching threshold Chl *a* 0.5 mg m^{-3}) for groups of open water polygons (SW, BIT, TIB, SE), polygons with seasonal sea ice cover (HD, SvS, SvN, SEB, CB, GB, NE), and the northern polygons with most sea ice (FVT, StAT, FJL) over the time series 1998–2017. See Fig. 1 for location and legend to Fig. 3 for name abbreviations of the polygons.

2000–2017 at the FB section (Fig. 8B) show that the seasonal dynamics and magnitude of the satellite Chl *a* concentration was highly correlated with the *in situ* Chl *a* concentration in the upper 20 m (R^2 = 0.63).

Nitrate reached its maximum concentration (average of 0–20 m stratum), about 9–10 mmol m^{-3}, in mid-March due to winter mixing (Fig. 8A, B). The concentration decreased to very low levels by August (~1 mmol m^{-3}) and increased again in October when nutrients were replenished due to autumn mixing. Nitrate concentrations reached winter conditions by November.

Mesozooplankton biomass dynamics followed that of spring phytoplankton Chl *a* with a lag of about one month (Fig. 8C, D). Mesozooplankton biomass peaked in July-August (~10 g dry wt. m^{-2}) and was low during winter months (<4 g dry wt. m^{-2}). The average mesozooplankton biomass in May was somewhat higher during 2000–2017 than during 1987–1999, at 7.0 and 4.6 g dry wt. m^{-2}, respectively. For the other months, the differences in biomass between time periods were less.

4.6. Net primary production

NPP of the whole Barents Sea showed substantial interannual variability, but generally increased significantly during the period 1998–2017 (Fig. 9A, $p < 0.001$) by 110% (based on fitted values). Average NPP for the whole Barents Sea was much lower in years 1998–2008 than in the more recent decade of 2009–2017 (65 and 92 Tg C $year^{-1}$, respectively). NPP increased significantly in all polygons

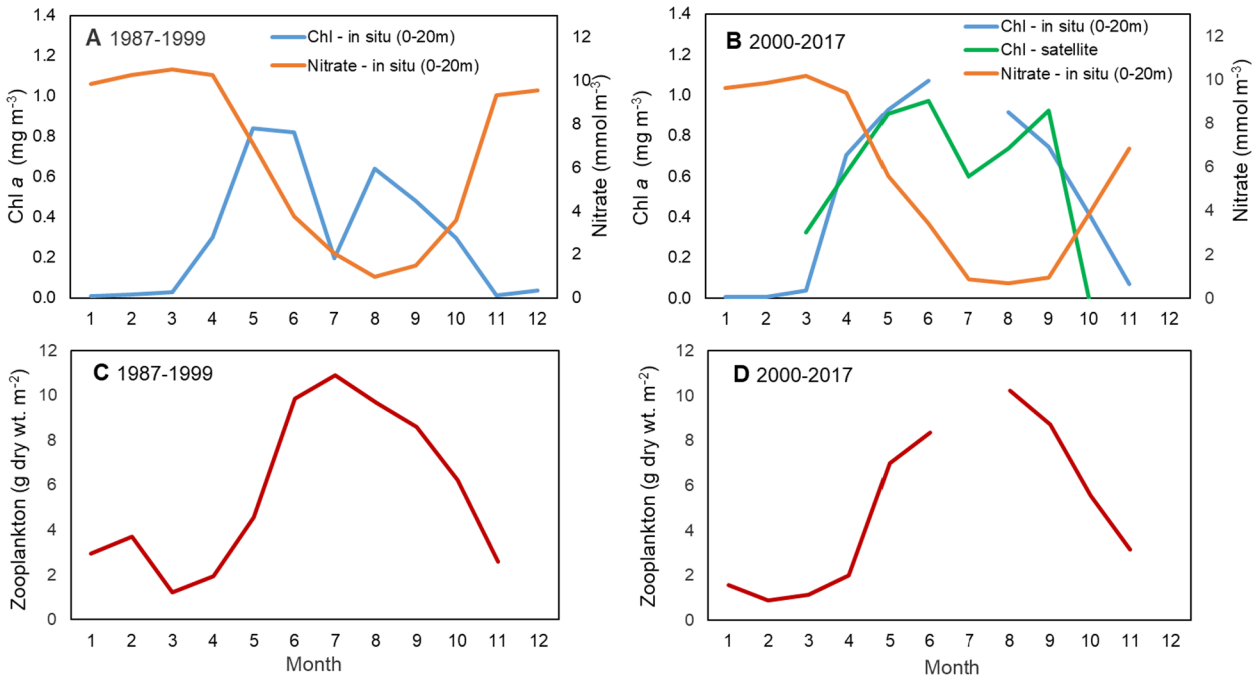

Fig. 8. Chl *a* and nitrate concentrations (0–20 m) (A, B) and mesozooplankton biomass (over the water column) (C, D) at the FB section for the periods 1987–1999 (A, C) and 2000–2017 (B, D). Satellite Chl *a* data (B) are for the period 2000–2017 only.

during the study period ($p < 0.05$). The most pronounced increase in NPP was in the eastern regions, North East and Pechora Sea polygons, by 377% and 161%, respectively (Fig. 9B, $p < 0.001$). NPP in the central and northern polygons also increased strongly over the years (Fig. 9C, D, $p < 0.01$), but production values were low compared to the southern and eastern regions. NPP also increased in the polygons of the southwestern region (e.g. SW, TIB, HD), but the increase was not that strong as in northern and eastern polygons, even though NPP values were comparatively high in most of the southwestern polygons at the end of the study period (e.g. > 5 Tg C in SW and TIB).

When considering the NPP standardized per unit surface area, the highest production (about 70–90 g C m^{-2} $year^{-1}$) occurred in the southern open water (or mostly open water) polygons (SW, BIT, TIB, SE, SEB) (Fig. 10). The NPP declined from south to north, to a level of 10–20 g C m^{-2} $year^{-1}$ for the northern and most strongly ice-influenced polygons (FVT, FJL, StAT). When normalized to area of open water by the end of the productive season (which is the maximum area with data obtained from the satellites), the NPP still declined from south to north but less pronounced, from about 70–90 g C m^{-2} $year^{-1}$ in open water polygons to a level of about 40 g C m^{-2} $year^{-1}$ for the northernmost polygons (Fig. 10). The mean rate of annual NPP for the whole Barents Sea (averaged across all polygons) was 48.0 g C m^{-2} $year^{-1}$ based on total area, and 60.0 g C m^{-2} $year^{-1}$ when expressed for open water area.

We found significant positive relationships between satellite-based NPP versus OWA and open water duration (OWD) over the time series 1998–2017 (Fig. 11; Table 1), suggesting that phytoplankton benefited from an extended ice free habitat, a prolonged growing season, or both. NPP was negatively correlated with the area of Arctic water and there was a strong positive trend with temperature on the Kola section (Table 1), likely reflecting the influence of ice free, warmer conditions.

A PCA analysis, examining how Barents Sea polygons were related to different biotic and abiotic variables, also shows that NPP is positively associated with OWA, OWD, and SST across polygons. Barents Sea polygons having high NPP, large OWA, and long OWD, are also characterized by strong changes in SST, high spring bloom Chl *a* peaks, earlier spring bloom peak days, and late fall bloom peak days, and to a weaker extent by lower mesozooplankton biomass (Fig. 12).

4.7. Mesozooplankton

4.7.1. Spatial variability in mesozooplankton biomass

The spatial distribution of mesozooplankton biomass displayed rather consistent patterns, as shown for some years with representative spatial coverage in Fig. 13. In general, the shallow bank areas (Central Bank, Great Bank, and the Thor Iversen Bank) had low mesozooplankton biomass (<4 g dry wt. m^{-2}). Another region with consistently low biomass was the Pechora Sea polygon in the southeastern Barents Sea. The areas influenced by the Atlantic currents in the west or the deeper basins, e.g. South Eastern Basin, generally had high biomass (~10 g dry wt. m^{-2}). In addition, high biomass (>10 g dry wt. m^{-2}) was commonly observed in northern polygons, e.g. Franz Victoria Trough, and northern areas of the North East polygon.

Data averaged over the years per polygon show (Table 2) that in general, the deep waters had higher biomass (>8.0 g dry wt. m^{-2}) than the shallow banks (<5 g dry wt. m^{-2}). The lowest average biomass values (<5.0 g dry wt. m^{-2}) were observed in the polygons from the eastern region, Pechora Sea and South East, in addition to the Central Bank and Great Bank (Table 2). The highest average biomass values (>10 g dry wt. m^{-2}) were observed in the Franz Joseph Land, Svalbard North, and Bear Island Trench polygons.

4.7.2. Interannual variability in mesozooplankton biomass

There was large interannual variability within polygons, shown by coefficients of variation (CV) varying from 0.51 to 1.50 across all samples per polygon (Table 2) and from 0.30 to 0.61 for yearly averages per polygon (Supplementary Table 5; Supplementary Table 6). The interannual variability in average mesozooplankton biomass for the whole Barents Sea (over all polygons) is illustrated in Fig. 14. The years 1994 and 1995 showed the highest average biomass during the study period (12.6 and 10.4 g dry wt. m^{-2}, respectively). Since year 2000, the biomass has been rather stable, varying from 5.8 to 8.4 g dry wt. m^{-2} (Fig. 14).

At the polygon level, the temporal variability of the annual mean values ranged by about a factor 5 (except for two polygons, SE and FVT, where values ranged by about a factor 30) (Fig. 15). The corresponding CV values for the annual polygon means ranged from 0.30 to 0.61

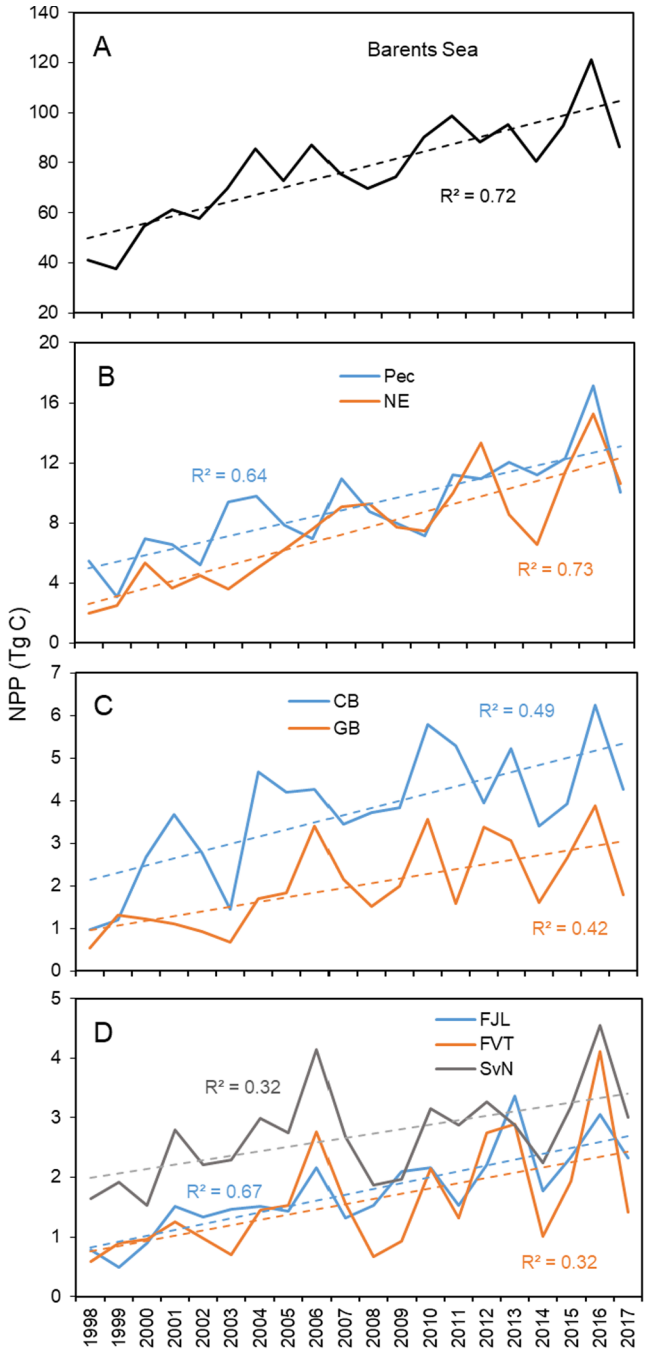

Fig. 9. Annual net primary production (satellite based NPP) for (A) the whole Barents Sea, (B) the Pechora Sea (Pec) and North East (NE) regions, (C) the Central Bank (CB) and Great Bank (GB) regions, and (D) the Franz Joseph Land (FJL), Svalbard North (SvN), and Franz Victoria Trough (FVT) regions. Note different scales on y-axis. R^2 in the figure refers to explanatory power of the regressions.

(Supplementary Table 6). In general, the polygons in the southwestern, northwestern, and eastern parts of the Barents Sea did not show clear trends over time (Fig. 15A, B, D). In contrast, the central region showed a decreasing trend in mesozooplankton biomass since early 2000, particularly in the Central Bank and Great Bank regions (Fig. 15C). The biomass was significantly lower in the years after 2004, compared to the years before, in the Great Bank (Mann–Whitney test, $p = 0.003$) and Central Bank ($p = 0.045$), while there was no significant difference between the two-time periods for the Thor Iversen Bank polygon ($p = 0.144$). Note that some of the polygon regions, specifically Svalbard North, St. Anna Trough, Franz Joseph Land, Pechora Sea, and South East, were poorly covered in some years (Supplementary Table 6). Another noteworthy observation is that the year 1994 had consistently high mesozooplankton biomass throughout our regions (with a delay to 1995 in some polygons), a special event that is currently under investigation.

4.7.3. Relationship with capelin stock

The Barents Sea capelin has undergone pronounced stock collapses and recoveries, with an apparent inverse relationship to mesozooplankton biomass (Fig. 14). When examining at a finer spatial scale (polygon level) over the whole study period, we see clear statistically significant negative relationships between annual average total mesozooplankton biomass and total capelin stock biomass, especially in central regions (Great Bank, Central Bank, and Thor Iversen Bank polygons) of the Barents Sea (Table 3). In areas with high capelin biomass, such as the Central Bank region, the negative relationship was strong, and capelin stock size explained ~50% of the interannual variability in total mesozooplankton biomass during the period 1989–2017 (Fig. 16, Table 3). Similar significant negative relationships, although with lower R^2, were observed at Thor Iversen Bank, Great Bank, and South West polygon regions over the whole study period (Fig. 16, Table 3). In the Bear Island Trench polygon, a negative trend between the two variables was observed, though not statistically significant (Table 3). The trends remain negative in all areas when considering a more recent time period (1996–2017, Table 3). However, the statistical significance of the negative relationship between capelin and mesozooplankton biomass disappeared, which is driven by the exclusion of earlier years showing very high mesozooplankton biomasses (1994, and partly 1995) when capelin biomass was very low (Figs. 14 and 16).

5. Discussion

5.1. Level of phytoplankton primary production

Primary production (PP) as a fundamental process in ecosystems is generally difficult to quantify. Measuring or estimating PP can be done principally with four different approaches and methods: i) incubation methods (classical ^{14}C and newer ^{13}C incorporations), ii) *in situ* changes in water mass chemistry (e.g., oxygen, carbonate system), iii) remote sensing (satellites, aircraft) algorithms, and iv) mathematical modelling. Part of the difficulty in estimating PP is the large spatial and temporal variability in rates of photosynthesis, which makes it challenging to integrate e.g. annual rates of PP for a large system like the Barents Sea. For the Barents Sea, several estimates of PP by different methods exist, which converge to suggest that the annual PP is about 100 g C m^{-2} on average, with higher values in the warmer Atlantic water in the south (100–150 g C m^{-2}), and lower values (20–70 g C m^{-2}) in northern, ice-covered waters (Hunt et al., 2013; Skjoldal et al., 2020; Wassmann et al., 2006a). Our satellite-derived estimates of NPP (e.g. Figs. 9A, and 11) are in broad agreement with these values reported in previous literature. They appear on the low side of previous estimates, which may reflect that our satellite-based algorithms give estimates closer to new production than gross PP (including regenerated production). This is supported by the close agreement between satellite-based NPP estimates and the estimates of new production based on depletion of nitrate concentrations at the FB section (e.g. Fig. 8). We note that our satellite-based NPP estimates would have missed part of sub-surface and ice edge phytoplankton blooms (see below), as well as NPP of ice algae. Hegseth (1998) found that the annual production of ice algae was about 5 g C m^{-2}, or about 20% of the total NPP, in the ice-covered waters of the northern Barents Sea. For the whole Barents Sea, ice algae contributed <3% of the NPP (Wassmann et al., 2006b).

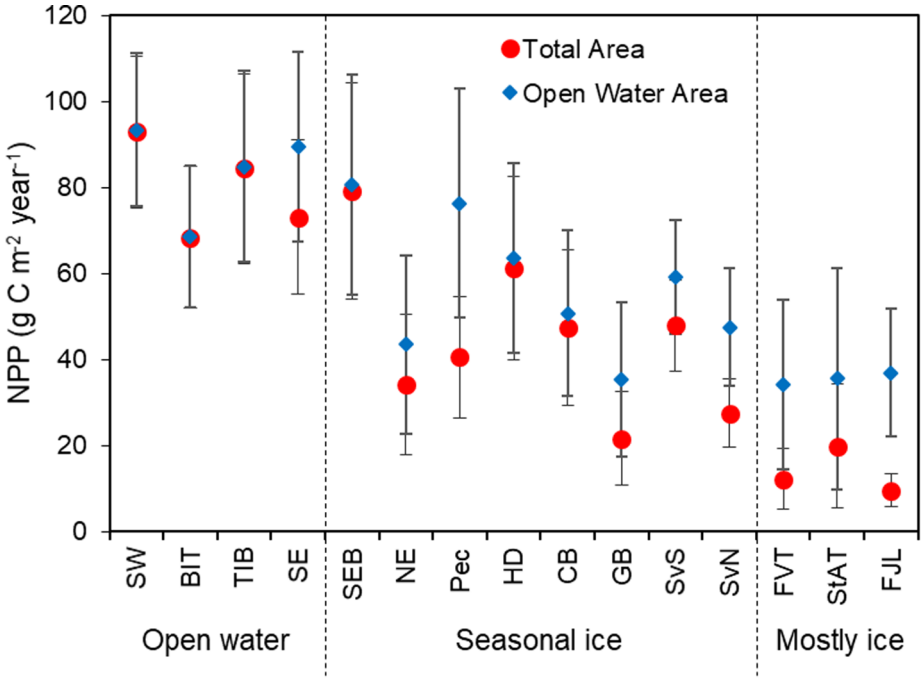

Fig. 10. NPP expressed as g C m^{-2} $year^{-1}$ for the different polygon regions. See Fig. 1 for location and legend to Fig. 3 for name abbreviations of the polygons. The two data points show NPP standardized by total polygon area (red) and by open water area (blue), respectively. Vertical error bars are +/− standard deviation for the data series 1998–2017. Note that the values for NPP for the South-East and Pechora Sea polygons were recalculated excluding the regions most influenced by river inflow (18% and 41% of the total area, respectively, see Materials and Methods).

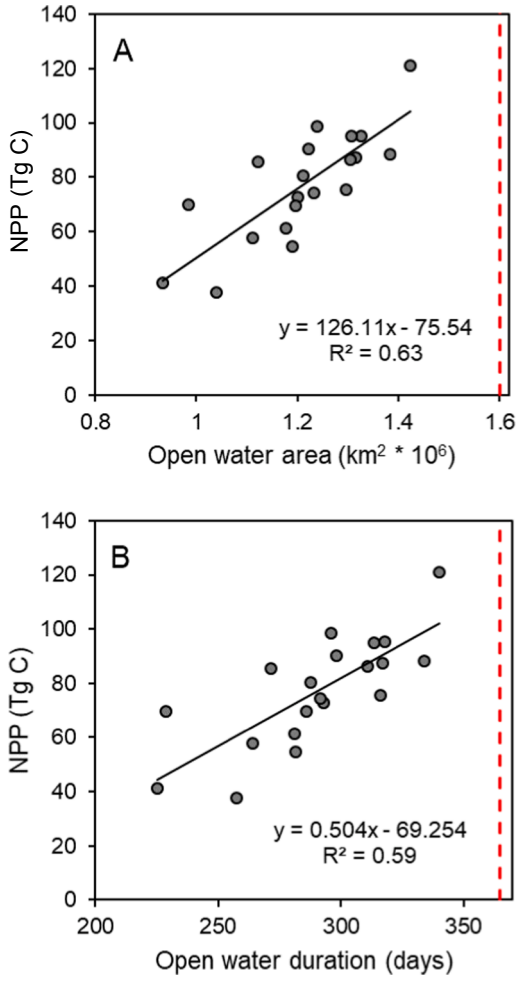

Fig. 11. Relationship between annual satellite-derived net primary production (NPP) and (A) open water area (OWA), and (B) open water duration (OWD) for the whole Barents Sea. The red dashed line indicates the maximum possible values of OWA and OWD (1.6 million km^2 and 365 days, respectively).

Table 1
Results of correlation analyses between annual satellite-derived net primary production (NPP) and open water area (OWA), open water duration (OWD), mesozooplankton biomass (Zoopl. Biom.), temperature on the Kola section (Kola temp.), and Arctic water area (ArW). p-values for statistical significance have been corrected for autocorrelation (p, see data analysis section for details) as well as for multiple comparisons (p*, after Bonferroni). Note, satellite-derived sea surface temperature (SST) and Chl *a* concentration have not been correlated with NPP as these variables were used to calculate NPP.

Correlation pairs	r	t	df	p	p*
NPP vs. OWA	0.79	3.33	6.61	0.014	0.068
NPP vs. OWD	0.77	3.15	6.95	0.016	0.081
NPP vs. Zoopl. Biom.	−0.20	−0.97	23.53	0.344	1.000
NPP vs. Kola temp.	0.68	2.79	8.93	0.021	0.105
NPP vs. ArW	−0.74	−3.15	8.29	0.013	0.065

5.2. Primary production increase over time

The satellite-based estimates show a clear increase in NPP of phytoplankton over the last two decades. This has been reported earlier (Dalpadado et al., 2014), but we extend and expand on those observations here, using newly reprocessed data from NASA (updated in 2018). For the whole Barents Sea, satellite-based NPP doubled during the 20-year period from 1998 to 2017, which corresponds to an increase of 2.9 Tg C per year (based on trend line in Fig. 9A). The observed increase in NPP is likely caused by reduced sea ice cover, which has a dual effect on PP: (i) more open water becomes available for phytoplankton, and (ii) the open water season is getting longer due to earlier melting of sea ice. Due to these effects, the annual NPP increased most strongly for polygons of the northern Barents Sea (mostly northeast), while moderate changes were observed for the southern Barents Sea (mostly southwest) that is influenced by Atlantic water and not ice covered. It should be noted that our results suggest that we are on course to a permanently ice-free Barents Sea: for the warmest, recent years (notably 2012 and 2016) we are approaching the total area of an ice-free Barents Sea as open water (Fig. 11A), and the full year as the open water duration (Fig. 11B). This means that we already are experiencing most of the increase in NPP that would be expected due to loss of sea ice in the Barents Sea.

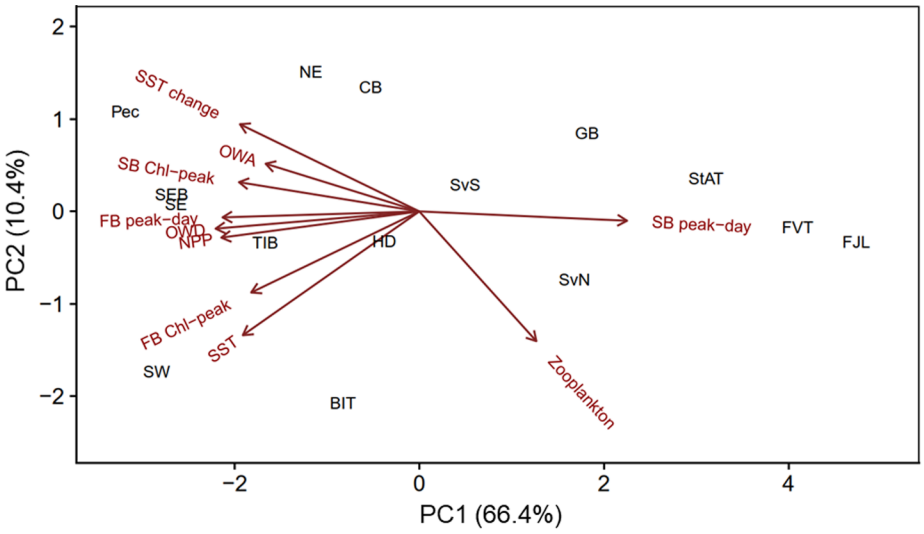

Fig. 12. PCA biplot showing how Barents Sea polygons are related to different biotic and abiotic variables. See Fig. 1 for location and legend to Fig. 3 for name abbreviations of the polygons. Variables: open water duration (OWD), open water area (OWA), sea surface temperature (SST), change in sea surface temperature (SST change, i.e. slope of regression SST vs. year), spring bloom Chl *a* peak (SB Chl *a*-peak), day of spring bloom Chl *a* peak (SB peak-day), fall bloom Chl *a* peak (FB Chl *a*-peak), day of fall bloom Chl *a* peak (FB peak-day), net primary production (NPP), and mesozooplankton biomass (zooplankton).

5.3. Spring blooms are occurring earlier

While there is some uncertainty in terms of absolute values, high resolution satellite data provide very valuable information on seasonal and spatial dynamics of the phytoplankton. Both the FB section and large scale spatial data show that phytoplankton spring bloom initiation varied by 1–3 months across polygons and years (see Figs. 6 and 7). The spring bloom initiation is driven by different stabilization mechanisms in the Atlantic water (thermocline formation) and ice-covered waters (ice melt; Skjoldal and Rey, 1989). Field studies in the 1980s demonstrated large interannual variability (by up to 4–6 weeks) in the timing of the spring bloom for both the Atlantic and sea-ice domains (Skjoldal et al., 1987; Skjoldal and Rey, 1989). Our more extensive data from satellite observations show interannual variability of similar magnitude.

In addition to the considerable interannual variability, there was a trend towards earlier blooming, which was evident in the northernmost polygons that are becoming more ice-free in summer. In these polygons, the phytoplankton spring bloom occurred earlier by nearly a month, with timing for the start of the spring bloom shifting forward from mid-June to mid-May (based on the trendline shown in Fig. 7), and the peak of the spring bloom from early July to early June (not shown). Open water and seasonally ice-covered areas in the central Barents Sea did not show a trend towards earlier blooming. Kahru et al. (2011), exploring surface Chl *a* for the Arctic Ocean by means of satellite data, found that the annual phytoplankton bloom maximum has advanced by up to 50 days in some areas, suggesting that earlier blooming may have consequences for the functioning of Arctic food webs and carbon cycling.

5.4. Are the satellites missing the ice edge bloom?

The peak Chl *a* values from this study show that the spring bloom was lower for the northern polygons than for the southern and central polygons (Fig. 5). This is somewhat surprising since it has been found that the ice edge bloom has similar or even higher peak Chl *a* concentrations compared to the spring bloom in the Atlantic water south of the ice (Rey et al., 1987; Skjoldal et al., 1987; Skjoldal and Rey, 1989; Strass and Nöthig, 1996). The ice edge bloom is usually of short duration (perhaps only around one week) and can be found as a narrow zone (a few tens of km) in the marginal ice zone (Sakshaug and Skjoldal, 1989; Skjoldal and Rey, 1989; Strass and Nöthig, 1996). The bloom itself, manifested as high Chl *a* in the surface layer, can take place inside the ice as this starts to break up and disintegrate (Skjoldal et al., 1987 – see their Fig. 8, Strass and Nöthig, 1996, see also Assmy et al., 2017).

Satellite observations of Chl *a* require open water since even low amounts of ice (down to 10% areal coverage) will confound the signal from the ocean color (Arrigo et al., 2012; Hill et al., 2013). Arrigo et al. (2012) observed strong phytoplankton blooms under Arctic sea ice, especially under melt ponds. Under-ice blooms have been observed in the Barents Sea as well (Kauko et al., 2019; Pavlov et al., 2017; Strass and Nöthig, 1996). It is therefore likely we are underestimating NPP in the ice-influenced polygons in the central and northern Barents Sea compared to the open water areas.

5.5. Length of the growing season

Since the satellite estimates may miss the ice edge bloom, the difference in Chl *a* level, and the time interval between spring and fall blooms as shown in Fig. 6, may be underestimated. Nevertheless, the presence of sea ice limits the growth of phytoplankton in spring, contributing to a shorter growing season for phytoplankton in the northern compared to the central and southern Barents Sea. The length of the growing season was found to be a main factor determining the annual PP across a wide range of locations with sea ice in the Arctic (Rysgaard et al., 1999). A shorter growing season is a main reason for lower NPP in the northern compared to the southern Barents Sea.

The transition to winter darkness progresses more rapidly at high latitudes (Sakshaug et al., 2009). For the Barents Sea, the largest change in daily incoming light takes place during September, with winter darkness arriving about one month earlier in the northern than in the southern Barents Sea (early October at 80°N versus early November at 70°N; Rey, 2004). Sea ice starts to form in the northern Barents Sea in early October, around the same time that light becomes too low for any substantial photosynthesis to take place. With the warming climate, sea ice formation is delayed and occurs after the seasonal PP has ceased. Therefore, sea ice plays little or no role for the termination of PP in autumn, and the longer growing season for phytoplankton is primarily or solely due to earlier melting of sea ice in spring.

5.6. Phytoplankton-zooplankton interactions

The magnitude, timing, and duration of the spring bloom play important roles for mesozooplankton development. The timing of the bloom may be the most important factor determining the life history strategies of herbivore mesozooplankton species (Falk-Petersen et al., 2009). The two dominant species are *Calanus finmarchicus* in the Atlantic water and *Calanus glacialis* in the Arctic water of the Barents Sea (Aarflot et al., 2018; Melle and Skjoldal, 1998; Tande, 1991). Egg

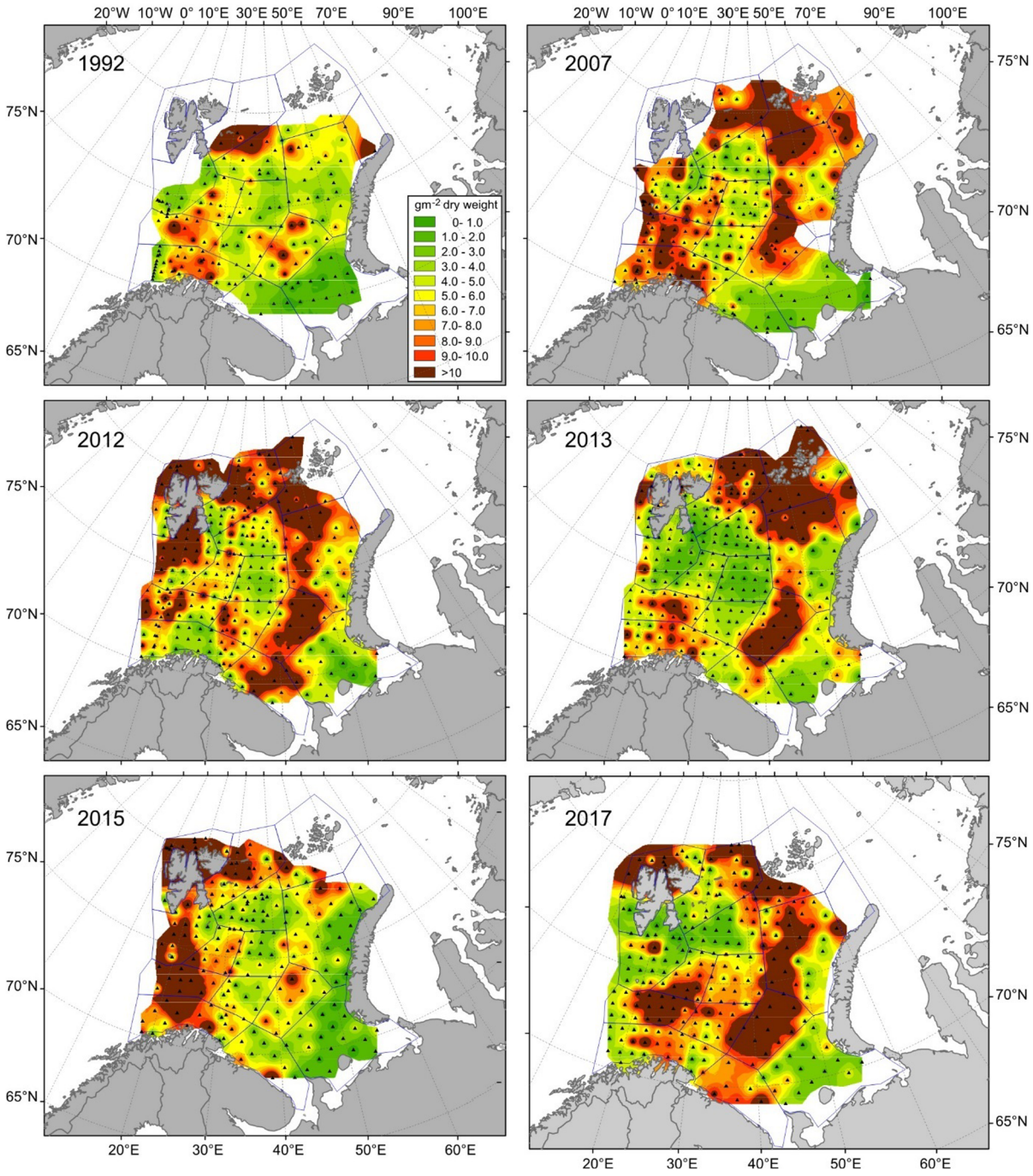

Fig. 13. Spatial distribution of total mesozooplankton biomass (near bottom to surface) of selected years from joint IMR and PINRO autumn ecosystem surveys. Note that zooplankton sampling on joint surveys took place after 2003 only; the data in 1992 were collected by IMR.

production by the two *Calanus* species depends to a large extent on phytoplankton as food (Hirche and Kosobokova, 2003; Melle and Skjoldal, 1998). The spring development of mesozooplankton is synchronized with the timing of the spring phytoplankton bloom.

Herbivorous zooplankton (notably the *Calanus* species) can crop the developing phytoplankton and thereby reduce the peak Chl *a* values in spring. This has been thought to be most effective with the slowly developing and prolonged spring blooms in Atlantic water compared to the more rapidly developing ice edge blooms driven by stability formation from ice melt (Skjoldal and Rey, 1989). Using data from the early 1980s (1979–1984), Skjoldal and Rey (1989) found that much more Chl *a* remained in the water column (normalized per unit nitrate consumed) in years with low copepod abundance compared to years with high copepod abundance. They explained this as an effect of variable grazing. It should be noted that the zooplankton showed particularly large changes and contrasts over these years (Dalpadado et al., 2003; Skjoldal et al., 1992).

Variable grazing pressure by mesozooplankton, both spatially and temporally, would be expected to influence Chl *a* levels. The effect of grazing is only indirectly incorporated in the satellite-based production estimates as lower Chl *a* due to grazing would result in lower NPP estimates. However, grazing may also lead to increased turnover in phytoplankton by stimulating regenerated production through consumer-driven nutrient recycling (Elser and Urabe, 1999; Nugraha et al., 2010).

The results from the FB section showed slightly advanced and

Table 2
Autumn mesozooplankton biomass pooled for all years (1989–2017) across all sampling stations in each of the polygons. Joint IMR and PINRO data. Mean values are given along with standard deviation (SD) and coefficient of variation (CV = SD/mean).

Polygon	No. Stations	Mean depth (m)	Zooplankton biomass (g dry wt. m^{-2})	SD	CV
Pechora Sea	297	108	3.22	4.82	1.50
South East	189	168	4.69	3.55	0.76
Central Bank	452	220	4.88	3.60	0.74
Great Bank	489	195	5.06	3.92	0.78
Svalbard South	544	178	6.12	6.68	1.09
Thor Iversen Bank	369	259	6.98	4.03	0.58
North East	513	219	7.36	4.87	0.66
South West	658	294	7.55	5.64	0.75
Hopen Deep	415	289	8.01	6.92	0.87
Franz Victoria Trough	335	243	8.56	6.28	0.73
Southeastern Basin	298	293	9.48	6.15	0.65
St. Anna Trough	40	256	9.65	5.38	0.56
Bear Island Trench	435	396	10.75	6.81	0.63
Svalbard North	161	344	10.80	10.75	1.00
Franz Joseph Land	90	250	11.18	5.75	0.51

prolonged zooplankton development for the period 2000–2017 compared to 1987–1999. Model simulations show that *C. finmarchicus* will most likely be unable to take full advantage of the predicted increase in Barents Sea NPP in the future, due to the predicted warmer temperature in the northern Barents Sea still being too low for successful generational development, and a mismatch between spawning and development of *Calanus* relative to the earlier phytoplankton peak in Arctic waters (Skaret et al., 2014). Further studies with high temporal and spatial resolution are needed to understand the response of mesozooplankton to earlier phytoplankton blooms in the Barents Sea.

5.7. Status of the phytoplankton and zooplankton communities in relation to capelin stock

Our results show that the increase in temperature and decrease in sea ice cover in the Barents Sea have led to larger open water areas, especially in the north and east, resulting in higher NPP by ~100% over the 20 years from 1998 to 2017. In recent years, the autumn mesozooplankton biomass has remained relatively stable (6–8 g dry wt. m^{-2}), even during time periods when capelin biomass was high (Fig. 14). If capelin exerted strong predation pressure on zooplankton in recent years, the stable zooplankton biomass would indicate favorable conditions for mesozooplankton production, partly counteracting the high predation levels.

However, the different *Calanus* species making up the bulk of the mesozooplankton have responded oppositely to temperature-related climatic fluctuations over the past 20 years, with an increase in proportion of Atlantic *C. finmarchicus* and a decrease in proportion of Arctic *C. glacialis* during the same period (Aarflot et al., 2018). Dalpadado et al. (2014) estimated trophic transfer efficiencies from phytoplankton to zooplankton of up to 26% in the Barents Sea ecosystem. In marine ecosystems, ~20% is considered a not uncommon transfer efficiency from plants to herbivores (Lalli and Parsons, 1993). The short and efficient energy transfer (phytoplankton → herbivorous mesozooplankton → capelin) in the Barents Sea ecosystem provides good feeding and growth conditions for higher trophic level organisms such as cod. The increased production at lower trophic levels over the last few decades probably had positive effects on the cod stock, which at present is at record high levels (ICES/WGIBAR, 2017, 2018).

Although we see an increase in the NPP over the years, we do not see a similar trend in the mesozooplankton biomass; in fact, there was a weak inverse relationship between the two variables (Table 1, Fig. 12). Top down processes imposed by pelagic planktivorous fish could impact the mesozooplankton significantly. We have focused on capelin, as it is the major predator on zooplankton in the Barents Sea, especially when the stock is at high levels (>3 million tons) (ICES, 2018). The extended time series up to 2017, covering a larger part of the Barents Sea than most previous studies, showed a significant negative relationship between zooplankton and capelin biomass (Table 3), with capelin explaining ~43% variability of the mesozooplankton biomass when

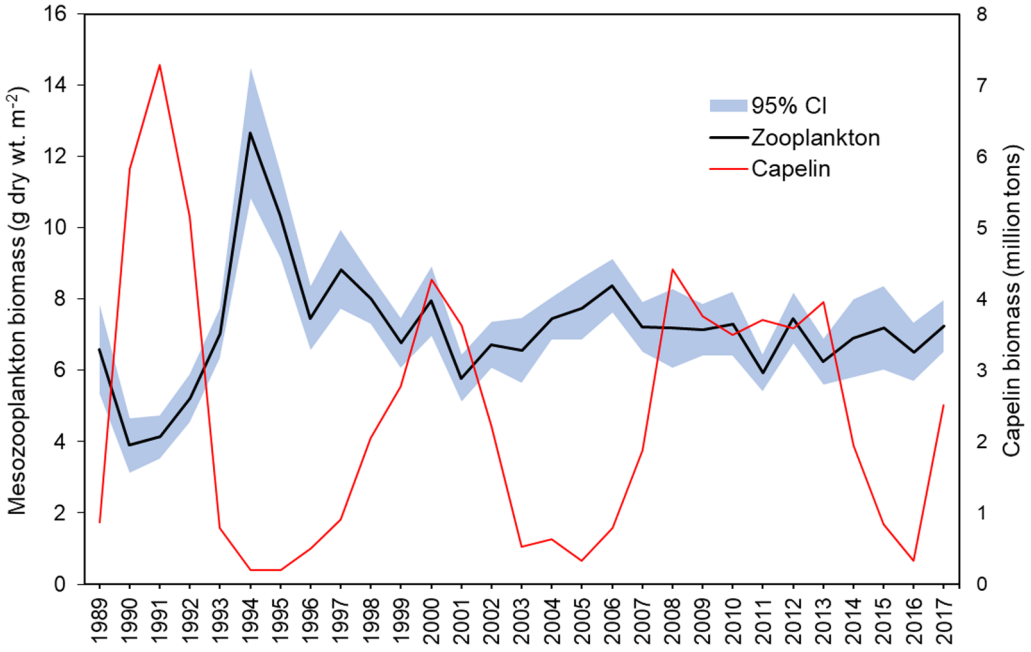

Fig. 14. Interannual variability in total mesozooplankton and total capelin biomass in the Barents Sea. Average zooplankton biomass over all polygons with 95% confidence interval shown as the blue shaded band. Total capelin stock biomass is from acoustic survey data (ICES 2018).

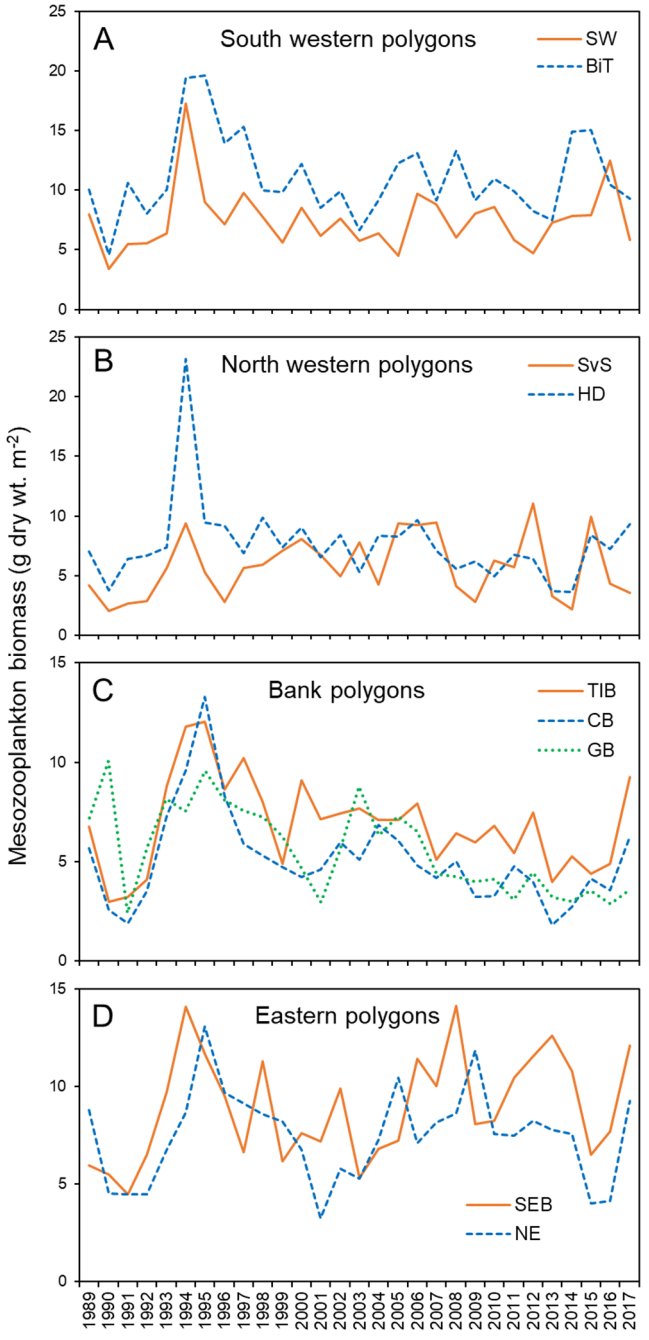

Fig. 15. Interannual variability of mesozooplankton biomass in selected polygons with good temporal coverage. A - South West (SW), and Bear Island Trench (BIT); B - Svalbard South (SvS), and Hopen Deep (HD); C - Thor Iversen Bank (TIB), Central Bank (CB), and Great Bank (GB); D - Southeastern Basin (SEB), and North East (NE). Polygons with poor temporal coverage are not shown (see Supplementary Table 6). Note different scales on y-axis.

considering the whole Barents Sea. Our results suggest that the negative relationship between zooplankton and capelin biomass has become weaker in recent years (Table 3), possibly due to good growth conditions (e.g. less ice and more NPP) for zooplankton. Despite the importance of capelin, herring may also have a strong impact on zooplankton at times in the southern parts of the Barents Sea due to its more southern distribution (up to 74°N) compared to capelin (mostly north of 74°N) (Gjøsæter et al., 2011; ICES, 2018). The annual diet of herring in the Barents Sea consists of about 50% copepods by weight, and the main feeding period of herring is in May-June, where the dominant prey is *C. finmarchicus* (Prokopchuk, 2019).

Table 3
Correlation analyses between mesozooplankton biomass and capelin stock biomass (both ln-transformed) in different areas of the Barents Sea for time series 1989–2017 and 1996–2017. p-values have been corrected for autocorrelation (Nc, the number of independent joint observations; see data analyses section for details).

Area	1989–2017				1996–2017			
	r	t	Nc	p	r	t	Nc	p
Whole Barents Sea	−0.66	−2.40	9.7	0.044	−0.27	−0.95	13.4	0.363
Central Bank	−0.71	−3.07	11.5	0.013	−0.42	−1.71	15.4	0.110
Thor Iversen Bank	−0.49	−2.87	28.2	0.008	−0.47	−1.75	12.8	0.181
Great Bank	−0.48	−2.63	24.8	0.015	−0.46	−1.60	11.4	0.144
South West	−0.50	−2.22	16.7	0.042	−0.17	−0.75	21.8	0.463
Bear Island Trench	−0.54	−2.04	12.3	0.068	−0.23	−0.95	17.6	0.354

5.8. Bank dynamics

The Barents Sea topography consists of troughs and basins, separated by shallower bank areas. Among the largest bank areas are the Central Bank, Great Bank, and the Thor Iversen Bank region. Perry et al. (1993) and Pedersen et al. (2005) have shown that the circulation around banks may create retention areas entrapping plankton for extended time periods. Therefore, banks can be considered as partially closed systems. The negative relationship between mesozooplankton and capelin persisted most clearly in the bank regions. One reason for this could be generally higher capelin biomass and thus predation rate in these regions since they are part of the core feeding area of capelin when they move north on their summer feeding migration from overwintering in the central Barents Sea (Gjøsæter, 1998). Zooplankton migration behaviour may also play a role in the bank regions. A study by Aarflot et al. (2019) showed that zooplankton depth distributions are highly related to zooplankton size and that the bottom constrains the vertical distributions, and hence, accessibility to planktivorous fish. Studies by Genin (2004) demonstrated that daily accumulations of zooplankton occur over topographies at shallow and intermediate depths when the topography blocks the morning descent of migrating zooplankton. The shallow depths may force zooplankton to remain in waters nearer the surface with more light, making them more vulnerable to predation compared to deeper regions in the Barents Sea (Aarflot et al., 2019). Overwintering in deeper waters by zooplankton such as *Calanus* copepods can be interpreted as a predator avoidance behaviour at the time of the year when PP is at its minimum (Aarflot et al., 2019; Bagøien et al., 2001; Melle et al., 2014).

Less ice cover and a longer production period in the Great Bank and Central Bank areas in recent years have likely provided improved feeding conditions for higher trophic levels. In the years 2008–2013, capelin probably exerted high predation pressure over an extended period in the bank regions due to high capelin biomass levels (>3.5 million tonnes). One likely consequence is the decline of the zooplankton biomass during this period (see Fig. 16). Feeding studies have shown that the stomach fullness of capelin is highest in the central regions of the Barents Sea (Dalpadado and Mowbray, 2013; ICES/WGIBAR, 2017, 2018). The findings from this study corroborate that the bank regions are important feeding grounds for capelin.

In the current study, we lack good spatial coverage of

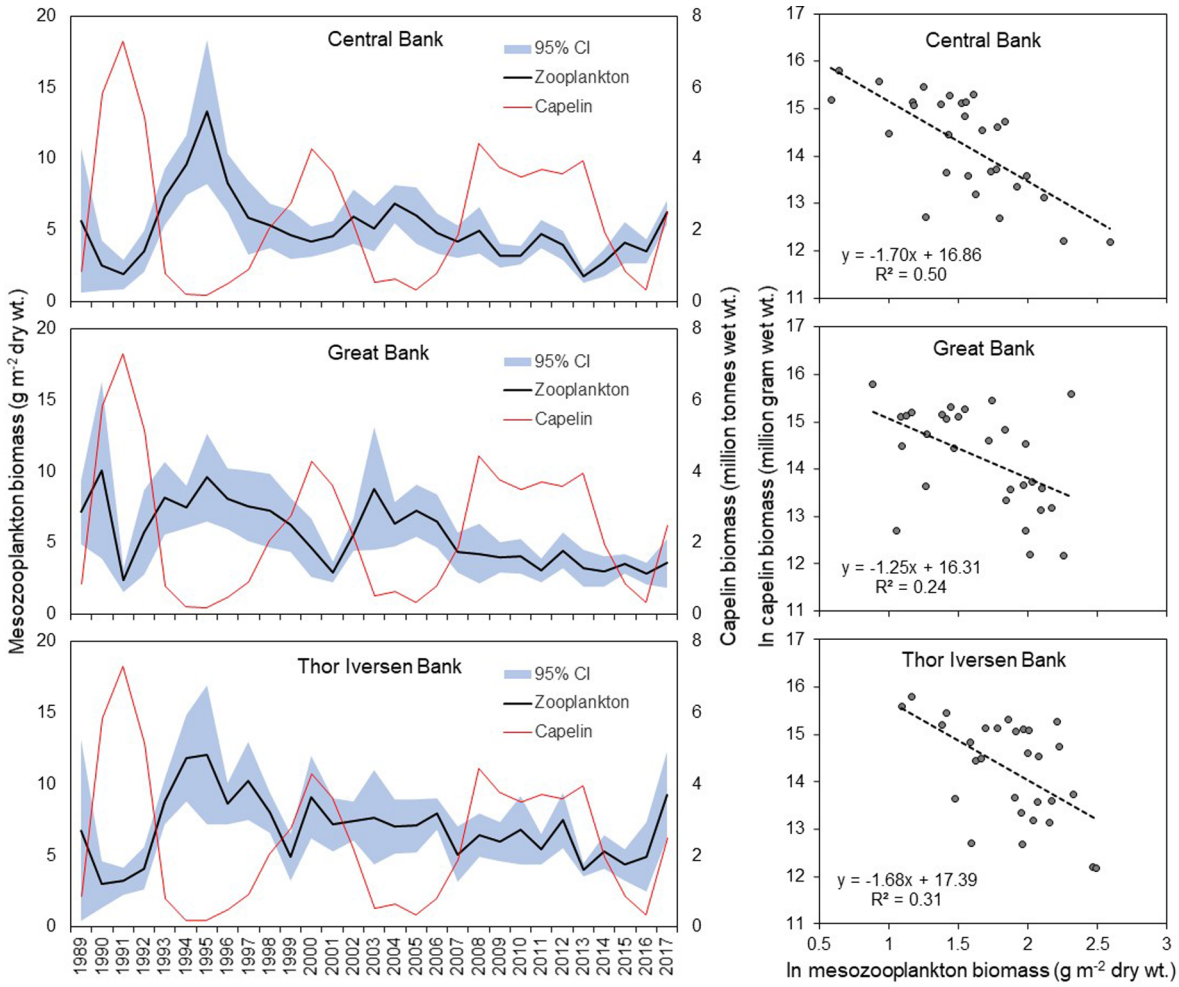

Fig. 16. Temporal dynamics (left panels) and relationships (right panels) between capelin and mesozooplankton biomass in the Central Bank, Great Bank, and Thor Iversen Bank area.

mesozooplankton in some polygons and years. Out of the 15 polygons, 10 polygons have reasonably good spatial and temporal coverage (see also Supplementary Table 6). The reason for the poor coverage is the variability in sea ice cover as well as limited sampling due to time constraints and survey priorities. However, the main capelin distribution areas generally overlap with the areas in which we have good coverage of mesozooplankton data. Therefore, the interactions between capelin and the mesozooplankton community we observe should reflect the dominant situation in the Barents Sea, suggesting top-down control of zooplankton by capelin predation.

5.9. Decrease in sea ice and its influence on the ecosystem

Sea ice algae are important components of the food web in Arctic and Antarctic ecosystems. Marine organisms that are dependent on sea ice are vulnerable to a reduction in ice extent (Arndt and Pavlova, 2005; Atkinson et al., 2004; Kohlbach et al., 2018). Understanding the role, i.e. the "hidden benefits", of ice algae in polar ecosystems is vital to predicting the impact of future sea ice decline on ecosystem functioning. Arrigo and van Dijken (2015) point out that the significant declines in sea ice cover observed in the recent decades, e.g. in the Arctic, has the potential to fundamentally alter marine ecosystems. The current study focuses mainly on the production in the open water and seasonally ice covered areas of the Barents Sea, the consequences of sea ice retreat, and how associated changes in NPP can impact organisms at higher trophic levels.

The strong decline in sea ice cover due to warming (e.g. Onarheim et al., 2018) seems to be the key driver of increasing phytoplankton NPP in recent years in the Barents Sea. Using remote sensing data, Oziel et al. (2017) observed two spatially distinct blooms in the Barents Sea, one along the ice edge and another in ice-free waters. These blooms are thought to be triggered by different stratification mechanisms: heating of the surface layer in ice-free waters and melting of sea ice along the ice edge (Sakshaug and Skjoldal, 1989; Skjoldal and Rey, 1989). The shift in relative importance and timing of these types of blooms may have consequences up the food web since synchrony of phenology between trophic levels is crucial for a productive environment. Several studies have shown shifts in plankton phenology as a response to warming. Thus, synchrony between abundance and timing of phytoplankton, zooplankton and larval fish is of importance for fish recruitment (Edwards and Richardson, 2004; Hays et al., 2015).

Climate-driven changes in the Arctic environment will result in winners and losers; some sub-Arctic species will shift their distribution ranges northwards into Arctic waters, while some currently abundant species will be displaced by these new migrants through competition or predation (Kelly, 2016) or simply by being unfit in new habitat conditions. The possible consequences may already be taking place. Using over three decades of continuous satellite observations, Neukermans

et al. (2018) observed that increased inflow of warmer Atlantic waters into the Barents Sea resulted in a striking poleward shift in the distribution of blooms of *Emiliania huxleyi*, a marine calcifying phytoplankton species (coccolithophorid). Makarevich et al. (2015) have also registered 38 new microalgae species for Kola Bay (the southern part of the Barents Sea) in the period 2001–2007. The results from our study show that phytoplankton dynamics in the ecosystem are changing rapidly and that these changes are driven mainly by bottom-up climatic processes such as diminishing sea ice cover. Habitat loss (decreasing sea ice) for some organisms and habitat gain (more open water area) for others may be anticipated due to large changes in sea ice coverage occurring in the ecosystem. In the western area of the Barents Sea, there are indications of an ongoing borealization of the zooplankton community, with a decreasing proportion of the Arctic copepod *C. glacialis* over the past 20 years and an increase in the Atlantic copepod *C. finmarchicus* (Aarflot et al., 2018). Even in the north-eastern Barents Sea (off Franz Josef Land) abundance and biomass of *C. finmarchicus* have increased during the 2000s (Orlova et al., 2014). The Arctic *C. glacialis*, which dominates the mesozooplankton in the northern Barents Sea, may depend on both ice algae and production by phytoplankton to reproduce successfully (Søreide et al., 2010), although *C. glacialis* seems to be able to survive in ice-free conditions in some Arctic regions (Daase et al., 2013). The Arctic pelagic amphipod *Themisto libellula* is known to have decreased during the warming period (Dalpadado et al., 2012; Stige et al., 2019), likely due to reduction in area dominated by Arctic water in the Barents Sea (Dalpadado et al., 2012; ICES/WGIBAR, 2018).

Simultaneously, Atlantic boreal euphausiid species, such as *Thysanoessa inermis* and *Meganyctiphanes norvegica*, have increased in numbers and biomass due to their northward expansion (Eriksen et al., 2017; Zhukova et al., 2009) as well as the rare species *Nematoscelis megalops* (Dolgov et al., 2018). Fish species such as Atlantic cod have also expanded their distribution northwards, reflecting the ongoing borealization of fish communities in the Barents Sea (Fossheim et al., 2015). Sea ice retreat and better light conditions may increase visual foraging ranges of fish living in the Arctic, such as polar cod, thereby intensifying top down control in this region (Langbehn and Varpe, 2017). It should be noted that the ongoing borealization, and subsequent decrease in area of Arctic water, will also impact higher trophic level organisms such as polar cod. In addition, the decrease in their prey (*C. glacialis* and *T. libellula*) will likely affect these stocks further. The decrease in stock size of polar cod observed in recent years, could be due to reduction in sea ice (Huserbråten et al., 2019) and key prey species.

Like the Arctic Ocean, studies from the Antarctic using fatty acid and stable isotope compositions of zooplankton and their food sources have shown that these organisms transfer significant amounts of carbon from ice algae into the pelagic system (Kohlbach et al., 2018). A negative interannual and spatial relationship observed between krill and copepods in Antarctica, has been interpreted in the context of predator-prey dynamics and food competition (Atkinson et al., 1999). Another example from the Antarctic is where two ecosystem components appear to respond in opposite manner to a decrease in sea ice. Densities of the major grazer Antarctic krill (*Euphausia superba)* decreased during the last century, while salps, e.g. the more warm water associated species *Salpa thompsoni,* appear to have increased in the southern part of their range (Atkinson et al., 2004). As food and the extent of winter sea ice are key factors regulating Antarctic krill populations, the decrease in sea ice and associated ice algae may have led to their decline. The changes among key species such as the Antarctic krill will have profound implications on the Southern Ocean food web (Atkinson et al., 2004 and references therein).

6. Conclusions

The Barents Sea is undergoing unprecedented changes in temperature and sea ice cover. Our study shows that diminishing sea ice leads to increasing NPP due to more open water and a prolonged growing season, thereby likely sustaining high zooplankton production in the system. Higher zooplankton biomass will probably have a positive impact on planktivorous fish and their predators. The fact that the Barents Sea currently supports some of the largest fish stocks in the world (ICES, 2018) indicates beneficial conditions for some inhabitants in the ecosystem. While Atlantic/boreal organisms have taken advantage of the warming by expanding their distribution and feeding areas, Arctic organisms will experience habitat loss, e.g. those species living in association with sea-ice (sympagic or adjacent). These changes will impact the biodiversity of the ecosystem towards more boreal and fewer Arctic species. Changes occurring in the Arctic are rapid and significant, as are the demand and necessity for integrated interdisciplinary long-term studies. Ecological observations and models of the Arctic Ocean are sparse, hence multi-disciplinary and multi-scale studies are needed to understand how diminishing sea ice and warming waters ultimately will alter Arctic marine ecosystems, including the health and behavior of key species on which Arctic people depend (Kelly, 2016).

7. Ethic statement

These studies were requested and given permission by the Norwegian government and Russian Federation under the bilateral agreement in the Barents Sea. Hence, any other specific permission was not required. The animals (fish, plankton) used in this work were collected from sea (their natural environment) in accordance with the national and international regulations compiled by the two states. No animals were kept in experimental conditions in this study.

Declaration of Competing Interest

The authors declare that they have no known competing financial interests or personal relationships that could have appeared to influence the work reported in this paper.

Acknowledgements

This study was funded by the Norwegian Research Council project TIBIA (Trophic interactions in the Barents Sea—steps towards an integrated ecosystem assessment, No. 228880), research project (No. 14923) under the Barents Sea Research Program at IMR and the WGIBAR project (Integrated Ecosystem Assessment for the Barents Sea, Nr. 15178). This work was inspired by the ICES Working Group on Zooplankton Ecology (WGZE) activities, under Terms of Reference (ToR E). We thank Karen Gjertsen for assistance with the layout of figures.

Appendix A. Supplementary data

Supplementary data to this article can be found online at https://doi.org/10.1016/j.pocean.2020.102320.

References

Aarflot, J.M., Skjoldal, H.R., Dalpadado, P., Skern-Mauritzen, M., 2018. Contribution of *Calanus* species to the mesozooplankton biomass in the Barents Sea. ICES J. Mar. Sci. 75, 2342–2354. https://doi.org/10.1093/icesjms/fsx221.

Aarflot, J.M., Aksnes, D., Opdal, A.F., Skjoldal, H.R., Fiksen, Ø., 2019. Caught in the daylight. Topographic constrains of zooplankton depth distributions. Limnol.

Oceanogr. 64, 849–859. https://doi.org/10.1002/lno.11079.
Aminot, A., Rey, F., 2000. Standard procedure for the determination of chlorophyll *a* by spectroscopic methods. ICES, Copenhagen, Denmark.
Arndt, C.E., Pavlova, O., 2005. Origin and fate of sea ice fauna in the Fram Strait and Svalbard area. Mar. Ecol. Prog. Ser. 301, 55–66. https://doi.org/10.3354/meps301055.
Arrigo, K.R., van Dijken, G.L., 2015. Continued increases in Arctic Ocean primary production. Prog. Oceanogr. 136, 60–70. https://doi.org/10.1016/j.pocean.2015.05.002.
Arrigo, K.R., van Dijken, G., Pabi, S., 2008. Impact of a shrinking Arctic ice cover on marine primary production. Geophys. Res. Lett. 35, L19603. https://doi.org/10.1029/2008GL035028.
Arrigo, K.R., Perovich, D.K., Pickart, R.S., Brown, Z.W., van Dijken, G.L., Lowry, K.E., Mills, M.M., Palmer, M.A., Balch, W.M., Bahr, F., Bates, N.R., Benitez-Nelson, C., Bowler, B., Brownlee, E., Ehn, J.K., Frey, K.E., Garley, R., Laney, S.R., Lubelczyk, L., Mathis, J., Matsuoka, A., Mitchell, B.G., Moore, G.W.K., Ortega-Retuerta, E., Pal, S., Polashenski, C.M., Reynolds, R.A., Schieber, B., Sosik, H.M., Stephens, M., Swift, J.H., 2012. Massive phytoplankton blooms under Arctic sea ice. Science 336, 1408. https://doi.org/10.1126/science.1215065.
Arrigo, K.R., van Dijken, G.L., Strong, A.L., 2015. Environmental controls of marine productivity hot spots around Antarctica. J. Geophys. Res. Ocean. 120, 5545–5565. https://doi.org/10.1002/2015JC010888.
Årthun, M., Nicholls, K.W., Makinson, K., Fedak, M.A., Boehme, L., 2012. Seasonal inflow of warm water onto the southern Weddell Sea continental shelf. Antarct. Geophys. Res. Lett. 39, L17601. https://doi.org/10.1029/2012GL052856.
Assmy, P., Fernández-Méndez, M., Duarte, P., Meyer, A., Randelhoff, A., Mundy, C.J., Olsen, L.M., Kauko, H.M., Bailey, A., Chierici, M., Cohen, L., Doulgeris, A.P., Ehn, J.K., Fransson, A., Gerland, S., Hop, H., Hudson, S.R., Hughes, N., Itkin, P., Johnsen, G., King, J.A., Koch, B.P., Koenig, Z., Kwasniewski, S., Laney, S.R., Nicolaus, M., Pavlov, A.K., Polashenski, C.M., Provost, C., Rösel, A., Sandbu, M., Spreen, G., Smedsrud, L.H., Sundfjord, A., Taskjelle, T., Tatarek, A., Wiktor, J., Wagner, P.M., Wold, A., Steen, H., Granskog, M.A., 2017. Leads in Arctic pack ice enable early phytoplankton blooms below snow-covered sea ice. Sci. Rep. 7, 40850. https://doi.org/10.1038/srep40850.
Atkinson, A., Ward, P., Brierley, A.S., Cripps, G.C., 1999. Krill-copepod interactions at South Georgia, Antarctica, II. *Euphausia superba* as a major control on copepod abundance. Mar. Ecol. Prog. Ser. 176, 63–79.
Atkinson, A., Siegel, V., Pakhomov, E.A., Rothery, P., 2004. Long-term decline in krill stock and increase in salps within the Southern Ocean. Nature 432, 100–103.
Bagøien, E., Kaartvedt, S., Aksnes, D.L., Eiane, K., 2001. Vertical distribution and mortality of overwintering *Calanus*. Limnol. Oceanogr. 46, 1494–1510. https://doi.org/10.4319/lo.2001.46.6.1494.
Bogstad, B., Gjøsæter, H., Haug, T., Lindstrøm, U., 2015. A review of the battle for food in the Barents Sea: cod vs. marine mammals. Front. Ecol. Evol. 3. https://doi.org/10.3389/fevo.2015.00029.
Carmack, E.C., Polyakov, I., Padman, L., Fer, I., Hunke, E., Hutchings, J., Jackson, J., Kelly, D., Kwok, R., Layton, C., Melling, H., Perovich, D., Persson, O., Ruddick, B., Timmermans, M.-L., Toole, J., Ross, T., Vavrus, S., Winsor, P., 2015. Towards quantifying the increasing role of oceanic heat in sea ice loss in the new arctic. America Meteorological Society. https://doi.org/10.1175/BAMS-D-13-00177.1.
Daase, M., Falk-Petersen, S., Varpe, Ø., Darnis, G., Søreide, J.E., Wold, A., Leu, E., Berge, J., Philippe, B., Fortier, L., 2013. Timing of reproductive events in the marine copepod *Calanus glacialis*: a pan-Arctic perspective. Can. J. Fish. Aquat. Sci. 70, 871–884. https://doi.org/10.1139/cjfas-2012-0401.
Dalpadado, P., Mowbray, F., 2013. Comparative analysis of feeding ecology of capelin from two shelf ecosystems, off Newfoundland and in the Barents Sea. Prog. Oceanogr. 114, 97–105. https://doi.org/10.1016/j.pocean.2013.05.007.
Dalpadado, P., Ingvaldsen, R., Hassel, A., 2003. Zooplankton biomass variation in relation to climatic conditions in the Barents Sea. Polar Biol. 26, 233–241. https://doi.org/10.1007/s00300-002-0470-z.
Dalpadado, P., Ellertsen, B., Johannessen, S., 2008. Inter-specific variations in distribution, abundance and reproduction strategies of krill and amphipods in the Marginal Ice Zone of the Barents Sea. Deep Sea Research Part II: Topical Studies in Oceanography 55, 2257–2265. https://doi.org/10.1016/j.dsr2.2008.05.015.
Dalpadado, P., Ingvaldsen, R.B., Stige, L.C., Bogstad, B., Knutsen, T., Ottersen, G., Ellertsen, B., 2012. Climate effects on Barents Sea ecosystem dynamics. ICES J. Mar. Sci. 69, 1303–1316. https://doi.org/10.1093/icesjms/fss063.
Dalpadado, P., Arrigo, K.R., Hjøllo, S.S., Rey, F., Ingvaldsen, R.B., Sperfeld, E., van Dijken, G.L., Stige, L.C., Olsen, A., Ottersen, G., 2014. Productivity in the Barents Sea - response to recent climate variability. PLoS One 9, e95273. https://doi.org/10.1371/journal.pone.0095273.
Dalsgaard, J., John, M.S., Kattner, G., Müller-Navarra, D., Hagen, W., 2003. Fatty acid trophic markers in the pelagic marine environment. Adv. Mar. Biol. 46, 225–340. https://doi.org/10.1016/S0065-2881(03)46005-7.
Dolgov, A.V., Orlova, E., Johannesen, E., Bogstad, B., Rudneva, G., Dalpadado, P., Mukhina, N., 2011. Planktivorous fishes. In: Jakobsen, T., Ozhigin, V.K. (Eds.), The Barents Sea. Ecosystem, Resources, Management. Half a Century of Russian-Norwegian Cooperation. Tapir Press, Trondheim, Norway, pp. 438–454.
Dolgov, A.V., Mikhina, A.S., Nesterova, V.N., Draganova, E.V., Kanischeva, O.V., Evseeva, E.V., Prokopchuk, I.P., Gordeeva, A.S., Zaitseva, K.A., 2018. Reference materials on distribution of euphausiids in the Barents Sea (2000–2015). PINRO Press, Murmansk, pp. 126 (in Russian).
Edwards, M., Richardson, A.J., 2004. Impact of climate change on marine pelagic phenology and trophic mismatch. Lett. Nat. 430, 881–884.
Elser, J.J., Urabe, J., 1999. The stoichiometry of consumer-driven nutrient recycling: theory, observations and consequences. Ecology 80, 735–751.
Eriksen, E., Skjoldal, H.R., Dolgov, A.V., Dalpadado, P., Orlova, E.L., Prozorkevich, D.V., 2016. The Barents Sea euphausiids: methodological aspects of monitoring and estimation of abundance and biomass. ICES J. Mar. Sci. 73, 1533–1544.
Eriksen, E., Skjoldal, H.R., Gjøsæter, H., Primicerio, R., 2017. Spatial and temporal changes in the Barents Sea pelagic compartment during the recent warming. Prog. Oceanogr. 151, 206–226. https://doi.org/10.1016/j.pocean.2016.12.009.
Eriksen, E., Gjøsæter, H., Prozorkevich, D., Shamray, E., Dolgov, A., Skern-Mauritzen, M., Stiansen, J.E., Kovalev, Yu., Sunnanå, K., 2018. From a single species towards monitoring of the Barents Sea ecosystem. Prog. Oceanogr. 166, 4–14. https://doi.org/10.1016/j.pocean.2017.09.007.
Falk-Petersen, S., Mayzaud, P., Kattner, G., Sargent, J.R., 2009. Lipids and life strategy of Arctic *Calanus*. Mar. Biol. Res. 5, 18–39. https://doi.org/10.1080/17451000802512267.
Fossheim, M., Primicerio, R., Johannesen, E., Ingvaldsen, R.B., Aschan, M.M., Dolgov, A.V., 2015. Recent warming leads to a rapid borealization of fish communities in the Arctic. Nat. Clim. Change 5, 673–677. https://doi.org/10.1038/nclimate2647.
Genin, A., 2004. Bio-physical coupling in the formation of zooplankton and fish aggregations over abrupt topographies. J. Mar. Syst. 50, 3–20. https://doi.org/10.1016/j.jmarsys.2003.10.008.
Gjøsæter, H., 1998. The population biology and exploitation of capelin (*Mallotus villosus*) in the Barents Sea. Sarsia 83, 453–496.
Gjøsæter, H., Dalpadado, P., Hassel, A., Skjoldal, H.R., 2000. A comparison of performance of WP2 and MOCNESS. J. Plankton Res. 22, 1901–1908. https://doi.org/10.1093/plankt/22.10.1901.
Gjøsæter, H., Ushakov, N.G., Prozorkevich, D.V., 2011. Capelin. In: Jakobsen, T., Ozhigin, V.K. (Eds.), The Barents Sea: Ecosystem, Resources, Management: Half a Century of Russian–Norwegian Cooperation. Tapir Academic Press, Trondheim, Norway, pp. 201–214.
Hagebø, M., Rey, F., 1984. Lagring av sjøvann til analyser av næringsalter. Fisken og Havet 4, 1–12 (in Norwegian).
Hassel, A., Skjoldal, H.R., Gjøsæter, H., Loeng, H., Omli, L., 1991. Impact of grazing from capelin (*Mallotus villosus*) on zooplankton: a case study in the northern Barents Sea in August 1985. In: Sakshaug, E., Hopkins, C.C.E., Øritsland, N.A. (Eds.), Proceedings of the Pro Mare Symposium on Polar Marine Ecology, Trondheim, 12–16 May 1990. Polar Research 10 (2), pp. 371–388.
Hays, G.C., Richardson, A.J., Robinson, C., 2015. Climate change and marine plankton. Trends Ecol. Evol. 20, 337–344.
Hegseth, E.N., 1998. Primary production of the northern Barents Sea. Polar Res. 17, 113–123.
Hill, S.L., Phillips, T., Atkinson, A., 2013. Potential climate change effects on the habitat of Antarctic krill in the Weddell Quadrant of the Southern Ocean. PLoS One 8, e72246. https://doi.org/10.1371/journal.pone.0072246.
Hirche, H.-J., Kosobokova, K., 2003. Early reproduction and development of dominant calanoid copepods in the sea ice zone of the Barents Sea. Need for a change of paradigms? Mar. Biol. 143, 769–781. https://doi.org/10.1007/s00227-003-1122-8.
Hunt, G.L., Blanchard, A.L., Boveng, P., Dalpadado, P., Drinkwater, K.F., Eisner, L., Hopcroft, R.R., Kovacs, K.M., Norcross, B.L., Renaud, P., Reigstad, M., Renner, M., Skjoldal, H.R., Whitehouse, A., Woodgate, R.A., 2013. The Barents and Chukchi Seas: comparison of two Arctic shelf ecosystems. J. Mar. Syst. 109–110, 43–68. https://doi.org/10.1016/j.jmarsys.2012.08.003.
Huserbråten, M.B.O., Eriksen, E., Gjøsæter, H., Vikebø, F., 2019. Polar cod in jeopardy under the retreating Arctic sea ice. Commun. Biol. 2, 407. https://doi.org/10.1038/s42003-019-0649-2.
ICES 2016. Report of the Arctic fisheries working group (AFWG), 19–25 April 2016, ICES HQ, Copenhagen, Denmark, ICES CM 2016/ACOM:06. 621pp.
ICES 2018. Report of the Arctic Fisheries Working Group, Ispra, Italy, 16–24 April 2018. ICES C.M. 2018/ACOM:06, 857pp.
ICES/WGIBAR, 2017. Report of the Working Group on the Integrated Assessments of the Barents Sea (WGIBAR). ICES CM 2017/SSGIEA:04, Murmansk, Russia.
ICES/WGIBAR, 2018. Interim Report of the Working Group on the Integrated Assessments of the Barents Sea (WGIBAR). ICES CM 2018/IEASG:04, Tromsø, Norway.
Ingvaldsen, R.B., Gjøsæter, H., 2013. Responses in spatial distribution of Barents Sea capelin to changes in stock size, ocean temperature and ice cover. Mar. Biol. Res. 9, 867–877. https://doi.org/10.1080/17451000.2013.775450.
Kahru, M., Brotas, V., Manzano-Sarabia, M., Mitchell, B.G., 2011. Are phytoplankton blooms occurring earlier in the Arctic? Glob. Chang. Biol. 17, 1733–1739. https://doi.org/10.1111/j.1365-2486.2010.02312.x.
Kauko, H.M., Pavlov, A.K., Johnsen, G., Granskog, M.A., Peeken, I., Assmy, P., 2019. Photoacclimation state of an Arctic underice phytoplankton bloom. J. Geophys. Res.: Oceans 124, 1750–1762. https://doi.org/10.1029/2018JC014777.
Kelly, B.P., 2016. How is diminishing Arctic sea ice influencing marine ecosystems? Arctic Answers. SEARCH. https://www.searcharcticscience.org/files/pyramid/assets/aa-003_june2017_ecosystems.pdf.
Kiørboe, T., 2013. Zooplankton body composition. Limnol. Oceanogr. 58, 1843–1850. https://doi.org/10.4319/lo.2013.58.5.1843.
Kohlbach, D., Graeve, M., Lange, B.A., David, C., Peeken, I., Flores, H., 2016. The importance of ice algae-produced carbon in the central Arctic Ocean ecosystem: food web relationships revealed by lipid and stable isotope analyses. Limnol. Oceanogr.

https://doi.org/10.1002/lno.10351.
Kohlbach, D., Graeve, M., Lange, B.A., David, C., Schaafsma, F.L., van Franeker, J.A., Vortkamp, M., Brandt, A., Flores, H., 2018. Dependency of Antarctic zooplankton species on ice algae produced carbon suggests a sea ice-driven pelagic ecosystem during winter. Global Change Biol. 24, 4667–4681.
Kvile, K., Dalpadado, P., Orlova, E., Stenseth, N., Stige, L., 2014. Temperature effects on *Calanus finmarchicus* vary in space, time and between developmental stages. Mar. Ecol. Prog. Ser. 517, 85–104. https://doi.org/10.3354/meps11024.
Langbehn, T.J., Varpe, Ø., 2017. Sea-ice loss boosts visual search: fish foraging and changing pelagic interactions in polar oceans. Global Change Biol. 23, 5318–5330. https://doi.org/10.1111/gcb.13797.
Lalli, C.M., Parsons, T.R., 1993. Biological Oceanography: An Introduction. Pergamon Press, Oxford.
Legendre, P., Legendre, L., 2012. Numerical Ecology, Third ed. Elsevier, Amsterdam, pp. 1006.
Leu, E., Søreide, J.E., Hessen, D.O., Falk-Petersen, S., Berge, J., 2011. Consequences of changing sea ice cover for primary and secondary producers in the European Arctic shelf seas: timing, quantity, and quality. Prog. Oceanogr. 90, 18–32.
Lind, S., Ingvaldsen, R.B., Furevik, T., 2018. Arctic warming hotspot in the northern Barents Sea linked to declining sea-ice import. Nat. Clim. Change 8, 634–639. https://doi.org/10.1038/s41558-018-0205-y.
Loeng, H., 1991. Features of the physical oceanographic conditions of the Barents Sea. Polar Res. 10, 5–18. https://doi.org/10.3402/polar.v10i1.6723.
Makarevich, P.R., Vodopyanova, V.V., Oleinik, A.A., 2015. Algal communities in the pelagic zone of Kola Bay. Structure and functional characteristics. Murmansk Marine Biological Institute, Kola Science Centre RAS. Rostov-on-Don, SSC RAS Publishers 192 pp (in Russian).
Melle, W., Skjoldal, H.R., 1998. Reproduction and development of *Calanus finmarchicus*, *C. glacialis* and *C. hyperboreus* in the Barents Sea. Mar. Ecol. Prog. Ser. 169, 211–228. https://doi.org/10.3354/meps169211.
Melle, W., Ellertsen, B., Skjoldal, H.R., 2004. Zooplankton: the link to higher trophic levels. In: Skjoldal, H.R. (Ed.), The Norwegian Sea Ecosystem. Tapir Academic Press, Trondheim, Norway, pp. 137–202.
Melle, W., Runge, J., Head, E., Plourde, S., Castellani, C., Licandro, P., Pierson, J., Jonasdottir, S., Johnson, C., Broms, C., Debes, H., Falkenhaug, T., Gaard, E., Gislason, A., Heath, M., Niehoff, B., Nielsen, T.G., Pepin, P., Stenevik, E.K., Chust, G., 2014. The North Atlantic Ocean as habitat for *Calanus finmarchicus*: environmental factors and life history traits. Prog. Oceanogr. 129, 244–284. https://doi.org/10.1016/j.pocean.2014.04.026.
Neukermans, G., Oziel, L., Babin, M., 2018. Increased intrusion of warming Atlantic water leads to rapid expansion of temperate phytoplankton in the Arctic. Global Change Biol. 24, 2545–2553. https://doi.org/10.1111/gcb.14075.
Nugraha, A., Pondaven, P., Tréguer, P., 2010. Influence of consumer-driven nutrient recycling on primary production and the distribution of N and P in the ocean. Biogeosciences 7, 1285–1305.
Onarheim, I.H., Eldevik, T., Årthun, M., Ingvaldsen, R.B., Smedsrud, L.H., 2015. Skillful prediction of Barents Sea ice cover. Geophys. Res. Lett. 42, 5364–5371. https://doi.org/10.1002/2015GL064359.
Onarheim, I.H., Eldevik, T., Smedsrud, L.H., Stroeve, J.C., 2018. Seasonal and regional manifestation of Arctic sea ice loss. J. Clim. 31, 4917–4932.
Orlova, E., Rudneva, G., Renaud, P., Elane, K., Todd, P., Savinov, V., Yurko, A., 2010a. Climate impacts on feeding and condition of capelin *Mallotus villosus* in the Barents Sea: evidence and mechanisms from a 30-year data set. Aquat. Biol. 10, 105–118. https://doi.org/10.3354/ab00265.
Orlova, E., Boitsov, V., Nesterova, V., 2010b. The influence of hydrographic conditions on the structure and functioning of the trophic complex plankton-pelagic fishes-cod. Murmansk, Murmansk printing company, pp. 190.
Orlova, E.L., Boitsov, V.D., Ivshin, V.A., Dolgov, A.V., Nesterova, V.N., 2014. Formation of mesoplankton structure in the central and northeastern Barents Sea in the period of warming in the Arctic. In: Karasev, A.B. (Ed.), The Formation of Bioproductivity in the Northern Barents Sea in the Period of Warming in the Arctic. PINRO Press, Murmansk, pp. 34–65 (in Russian).
Oziel, L., Neukermans, G., Ardyna, M., Lancelot, C., Tison, J.-L., Wassmann, P., Sirven, J., Ruiz-Pino, D., Gascard, J.-C., 2017. Role for Atlantic inflows and sea ice loss on shifting phytoplankton blooms in the Barents Sea. J. Geophys. Res. Oceans. 122, 5121–5139. https://doi.org/10.1002/2016JC012582.
Pavlov, A.K., Taskjelle, T., Kauko, H.M., Hamre, B., Hudson, S.R., Assmy, P., Duarte, P., Fernández-Méndez, M., Mundy, C.J., Granskog, M.A., 2017. Altered inherent optical properties and estimates of the underwater light field during an Arctic under-ice bloom of *Phaeocystis pouchetii*. J. Geophys. Res.: Oceans 122, 4939–4961. https://doi.org/10.1002/2016JC012471.
Pedersen, S.A., Ribergaard, M.H., Simonsen, C.S., 2005. Micro- and mesozooplankton in Southwest Greenland waters in relation to environmental factors. J. Mar. Syst. 56, 85–112. https://doi.org/10.1016/j.jmarsys.2004.11.004.
Perry, R.I., Harding, G.C., Loder, J.W., Tremblay, M.J., Sinclair, M.M., Drinkwater, K.F., 1993. Zooplankton distributions at the Georges Bank frontal system: retention or dispersion? Cont. Shelf Res. 13, 357–383. https://doi.org/10.1016/0278-4343(93)90056-4.
Polyakov, I.V., Pnyushkov, A., Alkire, M., Ashik, I.M., Baumann, T.M., Carmack, E.C., Goszczko, I., Guthrie, J.D., Ivanov, V.V., Kanzow, T., Krishfield, R.A., Kwok, R., Sundfjord, A., Morison, J.H., Rember, R., Yulin, A., 2017. Greater role for Atlantic inflows on sea-ice loss in the Eurasian Basin of the Arctic Ocean. Science 356, 285–291. https://doi.org/10.1126/science.aai8204.
Prokopchuk, I., 2019. Feeding ecology of immature herring *Clupea harengus* in the Barents Sea. In: Shamray, E., Huse, G., Trofimov, A., Sundby, S., Dolgov, A., Skjoldal, H. R., Sokolov, K., Jørgensen, L. L., Filin, A., Haug, T., Zabavnikov, V. (Eds.), Influence of Ecosystem Changes on Harvestable Resources at High Latitudes. The Proceedings of the 18th Russian-Norwegian Symposium, Murmansk, Russia, 5–7 June 2018, IMR/PINRO Joint Report Series, No. 1-2019, pp. 151–160 (217 pp).
Pyper, B.J., Peterman, R.M., 1998. Comparison of methods to account for autocorrelation in correlation analyses of fish data. Can. J. Fish. Aquat. Sci. 55, 2127–2140. https://doi.org/10.1139/f98-104.
Quenouille, M.H., 1952. Associated Measurements. Butterworth, London.
R Core Team, 2018. R: A language and environment for statistical computing. R Foundation for Statistical Computing, Vienna, Austria. https://www.R-project.org/.
Reigstad, M., Carroll, J., Slagstad, D., Ellingsen, I., Wassmann, P., 2011. Intra-regional comparison of productivity, carbon flux and ecosystem composition within the northern Barents Sea. Prog. Oceanogr. 90, 33–46. https://doi.org/10.1016/j.pocean.2011.02.005.
Rey, F., Skjoldal, H.R., Slagstad, D., 1987. Primary production in relation to climatic changes in the Barents Sea. In: Loeng, H. (Ed.), The Effect of Oceanographic Conditions on Distribution and Population Dynamics of Commercial Fish Stocks in the Barents Sea. Institute of Marine Research, pp. 29–46.
Rey, F., 2004. Phytoplankton: the grass of the sea. In: Skjoldal, H.R. (Ed.), The Norwegian Sea Ecosystem. Tapir Academic Press, Trondheim, Norway, pp. 97–136.
Reygondeau, G., Beaugrand, G., 2011. Future climate-driven shifts in distribution of *Calanus finmarchicus*. Global Change Biol. 17, 756–766.
Richardson, A.J., 2008. In hot water: zooplankton and climate change. ICES J. Mar. Sci. 65, 279–295.
Rysgaard, S., Nielsen, T., Hansen, B., 1999. Seasonal variation in nutrients, pelagic primary production and grazing in a high-Arctic coastal marine ecosystem, Young Sound, Northeast Greenland. Mar. Ecol. Prog. Ser. 179, 13–25. https://doi.org/10.3354/meps179013.
Sakshaug, E., 2004. Primary and secondary production in the Arctic Seas. In: Stein, R., Macdonald, R.W. (Eds.), The Organic Carbon Cycle in the Arctic Ocean. Springer, Berlin-Heidelberg, pp. 363.
Sakshaug, E., Skjoldal, H.R., 1989. Life at the ice edge. Ambio 18, 60–67.
Sakshaug, E., Johnsen, G., Kristiansen, S., von Quillfeldt, C., Rey, F., Slagstad, D., Thingstad, F., 2009. Phytoplankton and primary production. In: Sakshaug, E., Johnsen, G., Kovacs, K. (Eds.), Ecosystem Barents Sea. Tapir Academic Press, Trondheim, Norway, pp. 167–208.
Skagseth, Ø., Furevik, T., Ingvaldsen, R., Loeng, H., Mork, K.A., Orvik K.A., Ozhigin V., 2008. Volume and heat transports to the Arctic ocean via the Norwegian and Barents Seas. In: Dickson, R.R., Meincke, J., Rhines, P. (Eds.), Arctic-Subarctic Ocean Fluxes. pp. 45–64.
Skaret, G., Dalpadado, P., Hjøllo, S.S., Skogen, M.D., Strand, E., 2014. *Calanus finmarchicus* abundance, production and population dynamics in the Barents Sea in a future climate. Prog. Oceanogr. 125, 26–39. https://doi.org/10.1016/j.pocean.2014.04.008.
Skjoldal, H.R., Rey, F., 1989. Pelagic production and variability in the Barents Sea ecosystem. In: Sherman, K., Alexander, L.M. (Eds.), Biomass Yields and Geography of Large Marine Ecosystems. AAAS Selected symposium 111. American Association for the Advancement of Science, Washington, USA, pp. 241–286.
Skjoldal, H.R., Hassel, A., Rey, F., Loeng, H., 1987. Spring phytoplankton development and zooplankton reproduction in the central Barents Sea in the period 1979-1984. In: Loeng, H. (Ed.), The Effect of Oceanographic Conditions on Distribution and Population Dynamics of Commercial Fish Stocks in the Barents Sea. Institute of Marine Research, pp. 59–89.
Skjoldal, H.R., Gjøsæter, H., Loeng, H., 1992. The Barents Sea ecosystem in the 1980s: ocean climate, plankton, and capelin growth. ICES Mar. Sci. Symp. 195, 278–290.
Skjoldal, H.R., Dalpadado, P., Dommasnes, A., 2004. Food webs and trophic interactions. In: Skjoldal, H.R. (Ed.), The Norwegian Sea Ecosystem. Tapir Academic Press, Trondheim, Norway, pp. 447–506.
Skjoldal, H.R., Wiebe, P.H., Postel, L., Knutsen, T., Kaartvedt, S., Sameoto, D.D., 2013. Intercomparison of zooplankton (net) sampling systems: results from the ICES/GLOBEC sea-going workshop. Prog. Oceanogr. 108, 1–42. https://doi.org/10.1016/j.pocean.2012.10.006.
Skjoldal, H.R., Prokopchuk, I., Bagøien, E., Dalpadado, P., Nesterova, V., Rønning, J., Knutsen, T., 2019. Comparison of Juday and WP2 nets used in joint Norwegian-Russian monitoring of zooplankton in the Barents Sea. J. Plankton Res. 41, 759–769.
Skjoldal, H.R., et al., 2020. The Barents Sea Large Marine Ecosystem. In: Skjoldal, H.R. (Ed.), Descriptions of Arctic Marine Species and Ecosystems – Baseline Information for Assessments of Impacts of Climate Change and Human Activities. Arctic Monitoring and Assessment Programme (AMAP) and Institute of Marine Research, Norway (in press).
Stige, L.C., Dalpadado, P., Orlova, E., Boulay, A.-C., Durant, J.M., Ottersen, G., Stenseth, N.C., 2014. Spatiotemporal statistical analyses reveal predator-driven zooplankton fluctuations in the Barents Sea. Prog. Oceanogr. 120, 243–253. https://doi.org/10.1016/j.pocean.2013.09.006.
Stige, L.C., Eriksen, E., Dalpadado, P., Kotaro, O., 2019. Direct and indirect effects of sea ice cover on major zooplankton groups and planktivorous fishes in the Barents Sea (in press). ICES J. Mar. Sci. https://doi.org/10.1093/icesjms/fsz063.
Strass, V.H., Nöthig, E.-M., 1996. Seasonal shifts in ice edge phytoplankton blooms in the Barents Sea related to the water column stability. Polar Biol. 16, 409–422. https://

doi.org/10.1007/BF02390423.
Strickland, J.D.H., Parsons, T.R., 1972. A Practical Handbook of Seawater Analysis. Bulletin 157. Fish. Res. Bd. Can., Ottawa.
Søreide, J.E., Leu, E., Berge, J., Graeve, M., Falk-Pedersen, S., 2010. Timing of blooms, algal food quality and *Calanus glacialis* reproduction and growth in a changing Arctic. Global Change Biol. 16, 3154–3163. https://doi.org/10.1111/j.1365-2486.2010.02175.x.
Tande, K.S., 1991. *Calanus* in North Norwegian fjords and in the Barents Sea. Polar Res. 10, 389–408. https://doi.org/10.1111/j.1751-8369.1991.tb00661.x.
Vinje, T., 2009. Sea ice. In: Sakshaug, E., Johnsen, G., Kovacs, K. (Eds.), Ecosystem Barents Sea. Tapir Academy Press, Trondheim, Norway, pp. 65–82.
Wang, S.W., Budge, S.M., Iken, K., Gradinger, R.R., Sringer, A.M., Wooller, M.J., 2015. Importance of sympagic production to Bering Sea zooplankton as revealed from fatty acid-carbon stable isotope analyses. Mar. Ecol. Prog. Ser. 518, 31–50.
Wassmann, P., Slagstad, D., Riser, C.W., Reigstad, M., 2006a. Modelling the ecosystem dynamics of the Barents Sea including the marginal ice zone. J. Mar. Syst. 59, 1–24. https://doi.org/10.1016/j.jmarsys.2005.05.006.
Wassmann, P., Reigstad, M., Haug, T., Rudels, B., Carroll, M.L., Hop, H., Gabrielsen, G.W., Falk-Petersen, S., Denisenko, S.G., Arashkevich, E., Slagstad, D., Pavlova, O., 2006b. Food webs and carbon flux in the Barents Sea. Prog. Oceanogr. 71, 232–287.
Zhukova, N.G., Nesterova, V.N., Prokopchuk, I.P., Rudneva, G.B., 2009. Winter distribution of euphausiids (Euphausiacea) in the Barents Sea (2000–2005). Deep Sea Res. II 56, 1959–1967. https://doi.org/10.1016/j.dsr2.2008.11.007.